Sentinel-6 MF : F08 Reprocessing Calval Assessment

Reference : SALP-RP-MAO-OP-17710-CN
Issue : 1/ 1
Date : July 24, 2023

EUMETSAT
Eumetsat-Allee 1, D-64295 Darmstadt, Germany
Tel: +49 6151 807-7
Fax: +49 6151 807 555
http://www.eumetsat.int

Document Reference:	SALP-RP-MAO-OP-17710-CN
Date:	July 24, 2023
Issue	1.1

Project:	PROJECT NAME	
Title:	Sentinel-6 MF : F08 Reprocessing Calval Assessment	
	Name	**Company**
Author(s):	B. Courcol E. Cadier	CLS CLS
Approved by:	F. Bignalet-Cazalet	CNES
Application authorized by :	C. Martin-Puig	EUMETSAT

Change Log

Version	Date	Changes
1.0	17/07/2023	First Draft
1.1	24/07/2023	Eumetsat review taken into account

Acronyms

AMR	Advanced Microwave Radiometer
CLS	Collecte Localisation Satellites
CMEMS	Copernicus Marine Service
CNES	Centre National d'Etudes Spatiales
DUACS	Data Unification and Altimeter Combination System
DV	Default Value
ECMWF	European Centre for Medium-range Weather Forecasting
EUMETSAT	European Organisation for the Exploitation of Meteorological Satellites
ESA	European Space Agency
GIM	Global Ionosphere Maps
GDR	Geophysical Data Record
GMSL	Global Mean Sea Level
HR	High Resolution Mode, also called Synthetic Aperture Radar (SAR) or Delay Doppler Altimetry (DDA)
HRMR	High Resolution Microwave Radiometer
LR	Low Resolution Mode (=LRM)
LUT	Look-Up Table
MLE	Maximum Likelyhood Estimator
MQE	Mean Quadratic Error
MSS	Mean Sea Surface
NASA	National Aeronautics and Space Administration
NOAA	National Oceanic and Atmospheric Administration
NTC	Non Time Critical
PB	Processing Baseline
RMC	Range Migration Correction
SSH	Sea Surface Height
SSHA	Sea Surface Height Anomaly(=SLA)
SLA	Sea Level Anomaly(=SSHA)
SSB	Sea State Bias
STD	Standard Deviation
SWH	Significant Wave Height
WTC	Wet troposphere Correction

Table of Content

List of Figures

List of Tables

1 Introduction

Sentinel-6 is a collaborative Copernicus mission, implemented and co-funded by the European Commission, ESA, EUMETSAT and the USA through NASA and NOAA.

EUMETSAT is responsible for the Sentinel-6 operations as part of the Copernicus component of the EU Space Program. The Sentinel-6 Quality Assessment reports are generated by CNES as per EUMETSAT-CNES agreement in the context of Copernicus.

Since the launch of the Sentinel-6 MF satellite on 21st of November 2021, PDAP Processing Baseline (PB) has been updated several times following the satellite commissioning activities. This document presents the synthesis report concerning validation activities of Sentinel-6 MF PDAP 2023 reprocessing with PB F08. Sentinel-6 MF NTC products have been reprocessed using PB F08 until cycle 83 track 8. From cycle 83 track 9, PB F08 is used to compute operational NTC data.

The present global report deals with the complete reprocessed period of the Sentinel-6 MF mission, thanks to comparison with operational dataset. This reprocessing includes the addition of the numerical retracker in LR mode. A special focus on LR data is therefore presented in this report. The analysis is performed over ocean and using 1 Hz data.

This report is split into 3 main sections after this introduction describing the keys of the reprocessing campaign:

- First, the **data used** are presented.
- The **data coverage** and measurement validity issues are then presented.
- A synthesis of the **geophysical parameter derived from altimeter and radiometer** is exposed.

A second version, to be issued in September 2023, will add the analysis of the differences between Jason-3 and Sentinel-6 MF over the **tandem phase**, the impact of the reprocessing on the **GMSL**, and the compliance status to **system requirements**.

2 Data used and processing

2.1. Sentinel-6 MF F08 reprocessed data

Sentinel-6 MF data has been reprocessed with Processing Baseline F08 (PB) for Non-Time Critical (NTC) timeliness, for both LR (Low Resolution) and HR (High Resolution) modes.

The main change to this new F08 baseline is the **addition of numerical retracker (NR) retrievals in LR products for Ku band**. Numerical retracking allows accounting for the PTR shape evolution thanks to the use of in-flight PTRs. Please note that this new set of parameters does not replace but complement MLE4-derived parameters: NR and MLE4 retrievals are both included in LR products.

Other changes in PB F08 include :

- The update of the antenna aperture angle from 1.33° to 1.34°[1].
- The update of the total electron content (TEC) computation with a more appropriate scaling factor (0.881 instead of 0.925) to align the altimeter-derived TEC with the GPS-derived JPL GIM model.

Please note that an anomaly on NR SWH has been raised following the pre-operational validation of F08 data (AR 2620). Due to an implementation error, LR NR SWH 1Hz compression is done using sigma-composite whereas it should be done by direct averaging. The main impact of this error is that negative measurements of SWH are mapped to their absolute value at 20Hz and mixed to actual positive SWH during compression. 1 Hz NR SWH can be impacted up to 1 meter and has repercussions on some diagnostics detailed in this report. A patched version of PB F08 will be deployed at the end of summer 2023 and the anomaly will be retroactively corrected during the next reprocessing campaign.

A detailed description of the products can be found in the Sentinel-6 MF user handbook [2] and in the product notice [3].

The reprocessed data spans from 2020-12-17 at 22:17 to 2023-02-09 at 01:40, corresponding to the period from cycle 4 track number 14 to cycle 83 track number 8.

The analysis is performed over ocean and using 1 Hz data. For LR, both "ocean" retrackers were used, being MLE4 and NR, as well as the SAMOSA retracker in HR.

In the following assessment, the reprocessed dataset is referred as "REP" on the figures.

2.2. Sentinel-6 MF operational data used for comparison

From the beginning of the mission to 2022-08-15 (corresponding to cycle 65 pass 21), Sentinel-6 MF data were processed with the PB F06. No data with PB anterior to F06 is present in this study thanks to the 2022 F06 reprocessing campaign [1]. Data after 2022-08-15 were processed with PB F07.

The main changes brought by the PB F07 are :

- The availability of High Resolution Microwave Radiometer (HRMR) data in all radiometer products. All variables within the Level 2 altimeter products derived from the radiometer result from the combination

[1] In-flight operations have been conducted to better characterize the antenna aperture.

of AMR-C and HRMR data (ex: Wet Troposheric Correction).

- The usage of ECHO CAL as main source of CAL1.
- An update of the ionospheric correction filtering method. With this update, the filtered ionospheric correction became available over the Caspian Sea in the products, enabling SLA computation in this region.

Mode details on the PB F07 can be found in the associated product notice [4].

In the following assessment, the operational dataset is referred as "OPE" on the figures.

2.3. Jason-3 data used for comparison

Between 2020/12/17 to 2022/04/07 (cycle 4 to 51 for Sentinel-6 MF), Sentinel-6 MF and Jason-3 are flying in tandem formation on the same ground track with only 30 seconds apart, Jason-3 ahead of Sentinel-6 MF.

In this current report, Jason-3 GDR-F standard with MLE4 retracking was used to compare to Sentinel-6 MF reprocessed data. A detailed description of the products can be found in the Jason-3 product handbook [5].

Sentinel-6 MF PB F06 to F08 and Jason-3 GDR-F share the same standards in terms of geophysical corrections: same tide models, same mean surface height, etc. In particular :

- for the wind speed, Collard algorithm is used on both mission
- for the sea state bias, Sentinel-6 MF uses the same Sea State Bias parametrization as Jason-3 GDR-F, both in LR and in HR.

3 Data coverage and validity of measurements

This section consists in analyzing the availability of data for level 2 NTC products before and after the reprocessing. Furthermore the edited (invalidated) measurements are monitored and analyzed.

3.1. Missing measurements

Sentinel-6A data availability is improved thanks to F08 reprocessing. In LR, 7 tracks are recovered (cycle 4 passes 13, 15, 26 and 232 ; cycle 11 pass 1 and cycle 74 passes 35 and 68) and no new missing track is detected. Please note that cycle 74 pass 68 was recovered after the main reprocessed products generation and is not included in this report. In HR, 5 passes are recovered with the reprocessing (cycle 4 passes 13, 15 and 26, cycle 11 pass 1 and cycle 50 pass 251) and one pass is lost with the reprocessing (cycle 10 pass 254). However, this loss is minimal as this pass only contains 16 points in operational dataset.

Table 1 lists the total number of passes in the reprocessed data, and the number of passes with a different number of points with respect to the operational dataset, with thresholds of 1 and 500 (i.e. 8min and 20s). A few number of passes have less available points in the reprocessed dataset than in the operational dataset, respectively 28 in LR and 33 in HR. However, this data loss is marginal as the number of data points lost is of exactly 1 in all case except two : 16 points for cycle 10 pass 254 (already mentioned above), and 6 points cycle 25 pass 153 in LR. On the other hand, about three quarters of all passes in LR and HR have at least 1 more point in reprocessed than in operational. The reason is still under investigation. Once again, the number of points recovered per pass is in average low, typically 1 or 2. 24 passes in LR have more than 500 recovered points, as well as 11 passes in HR.

Parameter	LR	HR
Total number of passes in reprocessing	20066	20066
Number of passes with at least 1 more missing point wrt to operational dataset	28	33
Number of passes with at least 1 less missing point wrt to operational dataset	15297	14356
Number of passes with at least 500 more missing points wrt to operational dataset	0	0
Number of passes with at least 500 less missing points wrt to operational dataset	24	11

Table 1 – Number of passes with a different number of missing points in reprocessed wrt operational. This includes passes that are entirely missing.

The cyclic monitoring of available data for both dataset is presented in figure 1.

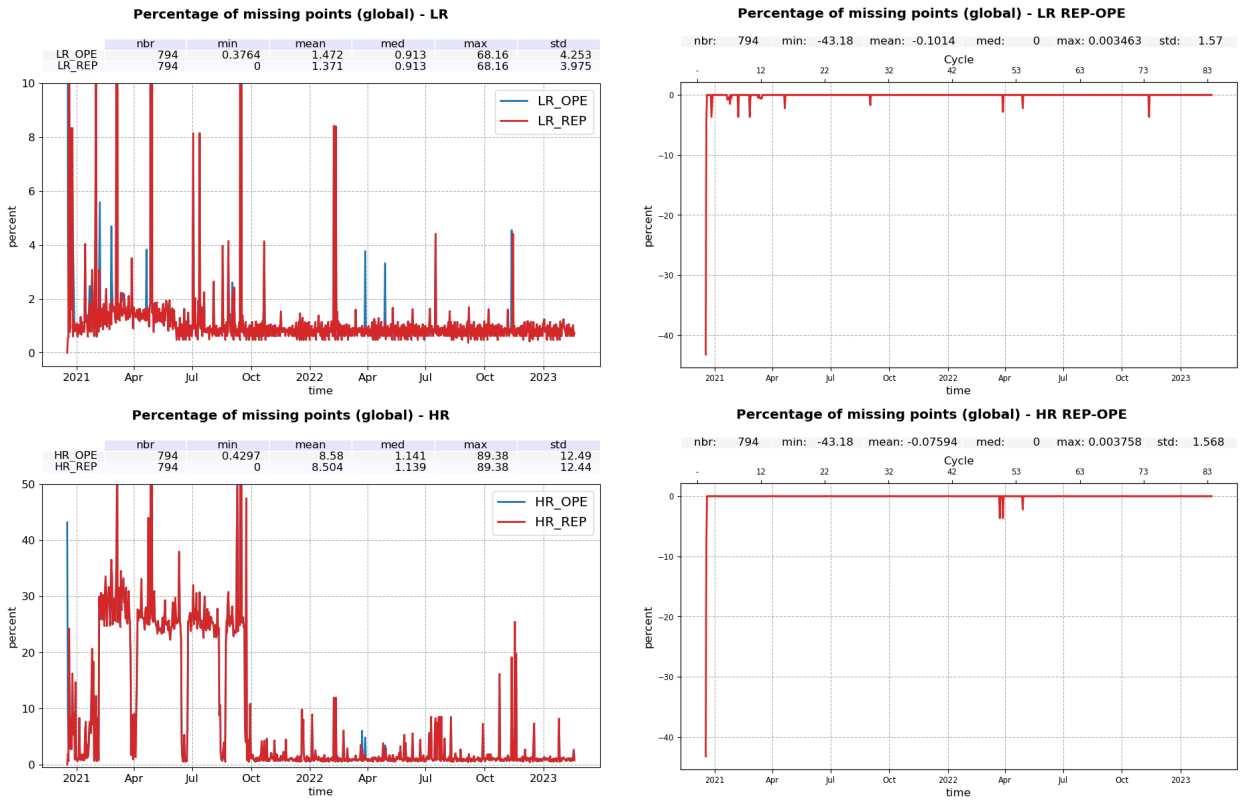

*Figure 1 – Percentage of missing data for the operational and reprocessed datasets (**left**) and their difference (**right**) for both LR (**top**) and HR (**bottom**). On the difference plots, positive values represent a loss of data with the reprocessing and negative values a gain of data thanks to the reprocessing.*

3.2. Wrong equator time in products

Products with erroneous equator time in their attributes are listed in tables 2 and 3. There are 4 products impacted in LR and 16 products impacted in HR. Impacted products are passes with significant missing segments that include the equator. In these cases, the equator times in the product attributes correspond to that of the previous pass. Please note that this issue was already present in PB F06 and F07 products.

Cycle	Pass	File name
4	82	S6A_P4_2__LR_STD__NT_004_082_20201220T140017_20201220T140200_F08.nc
16	120	S6A_P4_2__LR_STD__NT_016_120_20210420T011844_20210420T013649_F08.nc
17	82	S6A_P4_2__LR_STD__NT_017_082_20210428T114111_20210428T114302_F08.nc
35	8	S6A_P4_2__LR_STD__NT_035_008_20211021T015440_20211021T020322_F08.nc

Table 2 – LR products with erroneous equator time in attributes

Cycle	Pass	File name
5	31	S6A_P4_2__HR_STD__NT_005_031_20201228T121152_20201228T121613_F08.nc
7	228	S6A_P4_2__HR_STD__NT_007_228_20210125T004312_20210125T005322_F08.nc
10	225	6A_P4_2__HR_STD__NT_010_225_20210223T155007_20210223T161648_F08.nc
12	47	S6A_P4_2__HR_STD__NT_012_047_20210308T130058_20210308T132754_F08.nc
16	103	S6A_P4_2__HR_STD__NT_016_103_20210419T092305_20210419T093746_F08.nc
19	106	S6A_P4_2__HR_STD__NT_019_106_20210519T061140_20210519T061321_F08.nc
31	97	S6A_P4_2__HR_STD__NT_031_097_20210914T212341_20210914T214706_F08.nc
32	223	S6A_P4_2__HR_STD__NT_032_223_20210929T172516_20210929T173333_F08.nc
35	8	S6A_P4_2__HR_STD__NT_035_008_20211021T015440_20211021T020322_F08.nc
42	161	S6A_P4_2__HR_STD__NT_042_161_20220104T110513_20220104T113049_F08.nc
61	35	S6A_P4_2__HR_STD__NT_061_035_20220706T223407_20220706T225134_F08.nc
62	159	S6A_P4_2__HR_STD__NT_062_159_20220721T164316_20220721T170252_F08.nc
74	153	S6A_P4_2__HR_STD__NT_074_153_20221117T104819_20221117T105257_F08.nc
74	196	S6A_P4_2__HR_STD__NT_074_196_20221119T030533_20221119T032931_F08.nc
77	147	S6A_P4_2__HR_STD__NT_077_147_20221216T230637_20221216T232830_F08.nc

Table 3 – HR products with erroneous equator time in attributes

3.3. Edited measurements

3.3.1. Overview

The outlier detection or editing step of the Cal/Val process is applied to remove any measurement that is considered erroneous. Thus, it helps to refine the various metrics which are provided in the specific sections dedicated to the performance over the ocean. The definition of an erroneous measurement, and of the accepted error level on the final sea level anomaly is of course a trade-off between accuracy and data coverage. The monitoring of the percentage of valid and edited measurements also provides relevant information about the mission performances.

A series of editing criteria are used to detect outliers over ocean. This process is divided into 3 main parts:

- Removal of all measurements affected by sea-ice.
- Removal of all measurements which exceed defined thresholds on different parameters.
- Further checks on along-track SLA consistency.

For each step of the process, the number of outliers is routinely monitored at Cal/Val level. The number of removed data is used to detect processing anomalies which could be due to instrumental, geophysical or algorithmic changes. The process performed here is dedicated to ocean applications. Data over land are removed using a land/water mask prior to the analysis described in this section. The editing criteria have not been changed with the reprocessing.

The percentage of edited data per day for the operational and reprocessed dataset over ocean is monitored on figure 2. The overall percentage of edited data is very similar between operational and reprocessed datasets both in LR (11.86 % and 11.84 % respectively for MLE4) and HR (10.39 % and 10.41 %). The NR dataset shows slightly lower levels of edited data at 11.6 % (further details in section 3.3.5.).

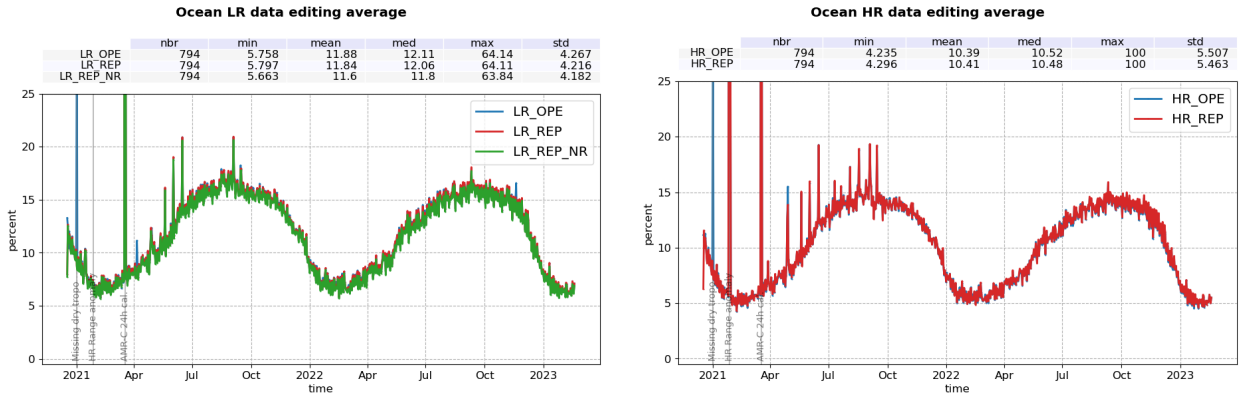

*Figure 2 – Percentage of valid measurement for the operational (blue) and reprocessed (red for MLE4 and SAMOSA, green for NR) datasets over ocean by day in LR (**left**) and HR (**right**).*

The main difference between operational and reprocessed datasets is a spike at cycle 5 in the operational data only (HR and LR). From passes 121 to 126 (included) of this cycle (i.e. from 01-01-2021 00:31:12.0 to 06:08:28.0), the dry tropospheric correction is set to default value in the operational products. This was caused by a missing meteo file, which has been recovered during the reprocessing.
Another notable spike that appear in all datasets in March 2021 is due to an AMR-C 24h warm calibration that impacted the ice flag, cf section 3.3.2.. Other spikes are statistical artifacts due to variations in the number of available measurements.

3.3.2. Rejection on ice detection

The first step of the editing process includes the removal of points with ice detection. The radiometer-derived ice flag ($rad\_sea\_ice\_flag$ in the products) is used to remove measurements affected by sea ice within the altimeter footprint.

The percentage of measurements edited on the ice flag criterion over ocean is monitored on the figure 3. There is no significant difference between operational and reprocessed datasets.

An AMR-C 24h warm target calibration conducted on the 17-18/03/2021 (on cycle 13 passes 20 to 45) caused the unavailability of ice flag over this period, resulting a spike in edited data.

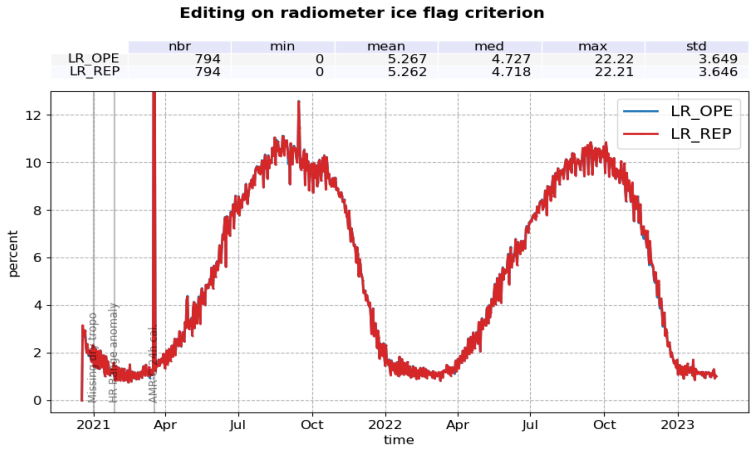

Figure 3 – Percentage of edited measurements on ice detection for the operational (blue) and reprocessed (red) datasets over ocean by day.

3.3.3. Rejection on thresholds criteria

Once the measurements corrupted by sea ice surfaces are identified, the quality of the parameters retrieved by the altimeter, as well as that of the geophysical corrections are checked with respect to defined thresholds. These thresholds and the corresponding percentage of corrupted measurements are detailed in table 4. For each of the listed parameters, the percentage of detected outliers is closely monitored cycle by cycle, day by day and pass by pass, by CLS Cal/Val routines.

Parameters	Min	Max	Unit	% rejected		
				LR MLE4	LR NR	HR
Sea surface height anomaly	-2	2	m	3.73/3.66	3.10	3.52/3.45
Sea surface height	-130	100	m	2.52/2.55	1.97	0.01/0.01
Nb measurements of range	10	N/A		0.14/0.16	0.00	0.1/0.01
Std. deviation of range	0	See (*)	m	2.72/2.82	0.58	0.62/0.91
Backscatter coefficient	LR: 7 HR: 10	LR: 30 HR: 35	dB	2.21/2.26	0.12	0.05/0.12
Nb measurements of sigma0	10	N/A		0.13/0.15	0.00	0.01/0.01
Std. deviation of sigma0	0	1	dB	3.87/4.13	2.32	0.70/0.85
Significant wave height	0	11	m	2.58/2.66	0.26	0.11/0.11
Altimeter wind speed	0	30	m.s-1	2.90/2.46	1.01	1.91/1.42
Sea State Bias	-0.5	0	m	2.23/2.25	0.02	0.04/0.04
Ionospheric correction filtered	-0.4	0.04	m	3.08/3.02	2.87	3.07/3.01
Square off nadir angle	-0.2	0.64	deg2	0.70/0.82	1.34	N/A
Equilibrium tide	-0.5	0.5	m	0.01/0.01	0.01	0.01/0.01
Combined atmospheric correction	-2	2	m	0.00/0.00	0.00	0.00/0.00
Dry tropospheric correction	-2.5	-1.9	m	0.07/0.04	0.04	0.07/0.04
Internal tide	-5	5	m	0.00/0.00	0.00	0.00/0.00
Ocean tide	-5	5	m	0.04/0.04	0.04	0.04/0.04
Pole tide	-15	15	m	0.00/0.00	0.00	0.00/0.00
Earth tide	-1	1	m	0.00/0.00	0.00	0.00/0.00
AMR wet tropospheric correction	-0.5	-0.001	m	0.19/0.19	0.20	0.19/0.19
Global statistics of edited measurements by thresholds				6.61/6.57	6.33	5.13/5.16

Table 4 – Table of parameters used for editing and the corresponding percentages of edited measurements for each parameter for Sentinel-6 MF LR and HR. In LR MLE4 and HR, first values correspond to operational data, second values to reprocessed data.

(*) The maximum threshold for range standard deviation is set as function of significant wave height as follows:
- In LR:
  - for SWH $\leq$ 2m : 0.192
  - for SWH > 2m : 0.018 * SWH + 0.156
- In HR:
  - for SWH $\leq$ 2m : 0.087
  - for SWH > 2m : 0.033 * SWH + 0.121

As table 4 shows, the percentage of edited points at this step is similar in LR MLE4 (6.6%) in the operational and reprocessed datasets. The percentage of edited points in LR NR is slightly lower at 6.3%. It is worth noting that parameters at default values are included in these threshold statistics, for they fail the boolean tests. Additionally, the majority of all edited points come from these default values rather than actual out of bound values, as can be seen in the daily monitoring of figure 4. On this monitoring, slightly different behaviours are observed between datasets. There are fewer criteria at default value in LR NR than in LR MLE4 reprocessed and in turn LR MLE4 operational. However, the opposite is true for criteria out of bounds. This indicates that more data are retrieved in NR (and in MLE4 reprocessed compared to MLE4 operational), but most of this additional data is of poor quality and then edited on threshold criteria.

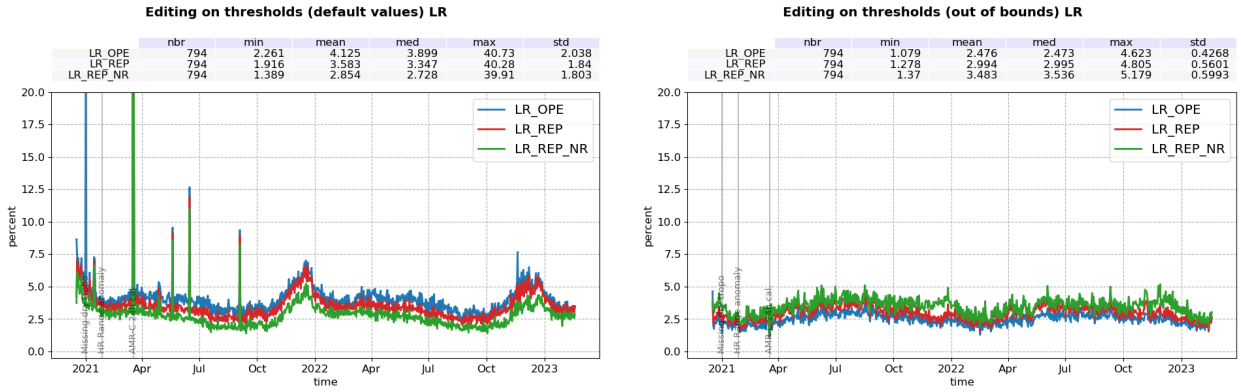

*Figure 4 – Percentage of edited measurements for the operational (blue) and reprocessed (red for MLE4 and green for NR) datasets over ocean by day based on parameters at default value (**left**) and out of bounds (**right**) in LR.*

3.3.4. Along-track SSHA consistency

Once the thresholds editing is applied, the consistency of the along-track sea surface height anomaly (SSHA) is checked. The statistics of the SSHA by pass are computed, with a selection that excludes zones of high geophysical variability. If the mean or the standard deviation is higher than a given threshold, the entire pass is edited. This process is repeated for a stricter set of selection and thresholds. The details are listed in table 5.

Parameters	Set 1	Set 2
Selection		
Bathymetry	<-1000m	<-1000m
Coastal distance	>100km	>100km
Oceanic variability	<0.3m	<0.1m
Min number of measurements	3	200
Thresholds		
Mean (absolute value)	0.3m	0.15m
STD	0.4m	0.2m

Table 5 – Table of parameters used for the editing on the SSHA pass statistics. These parameters are identical in HR and LR.

The percentage of edited points based on SSHA pass statistic is presented in figure 5. There is only one occurrence of this happening, at the cycle 20, passes 182 and 183 (01-06-2021 03:18:11.0 to 05:10:35.0), for all datasets. An issue have been found in the corresponding PTFA file, and new corrected products have been generated with PB F08 for both LR and HR. These new files have not been included in the present analysis.

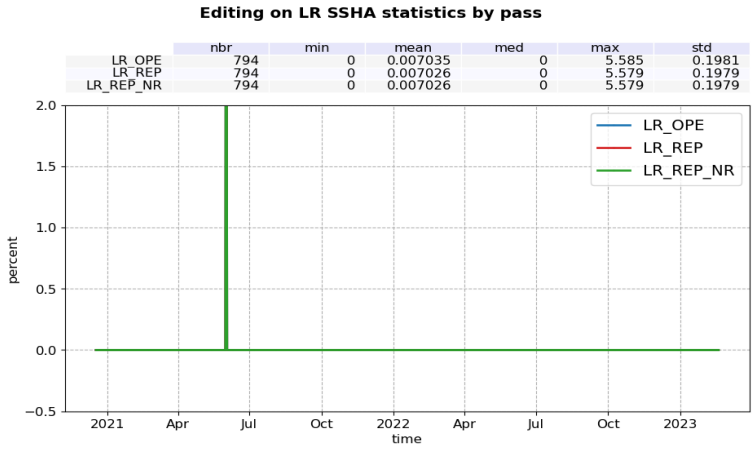

Figure 5 – Percentage of edited measurements on SSHA pass statistics for the operational (blue) and reprocessed (red) datasets over ocean by day in LR

3.3.5. Comparison between LR MLE4 and LR NR

This section focuses on the difference between LR reprocessed MLE4 and LR NR retrievals in terms of editing. The daily monitoring of data valid in MLE4 and not in NR is presented on the left panel of figure 6, while the monitoring of data valid in NR and invalid in MLE4 is presented on the right panel. The MLE4/NR differences are stable in time:

- 0.1 % of ocean data is edited in NR and not in MLE4, and is mostly located in high rain areas as seen on figure 7 (left panel).
- 0.4 % of ocean data is edited in MLE4 and not in NR, and is mostly located in low SWH areas as seen on figure 7 (right panel). This is linked to the anomaly on NR SWH (AR 2620) resulting in the absence of negative waves in NR. This negative waves are edited on a threshold criterion in MLE4 and thus not in NR (cf table 4).

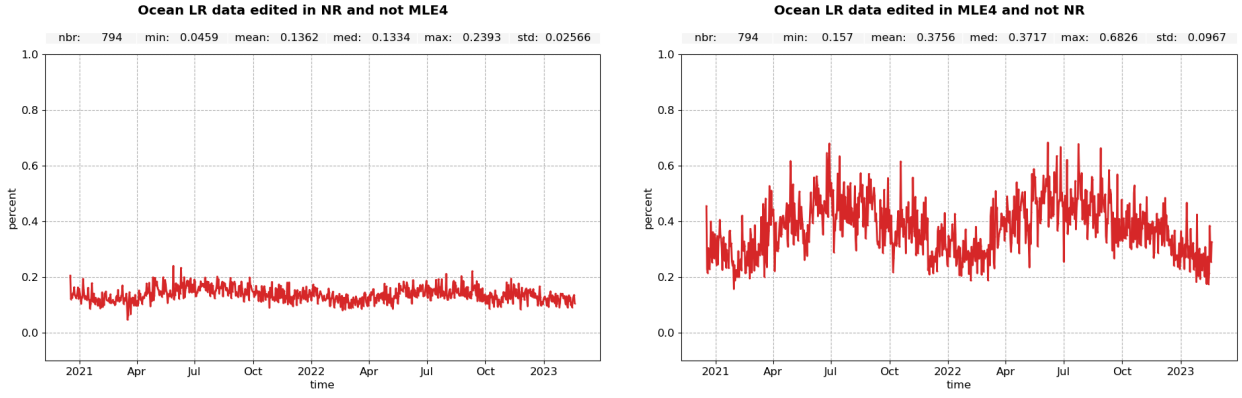

*Figure 6 – Percentage of edited reprocessed measurements per day in NR that are valid in MLE4 (**left**) and in MLE4 that are valid in NR (**right**).*

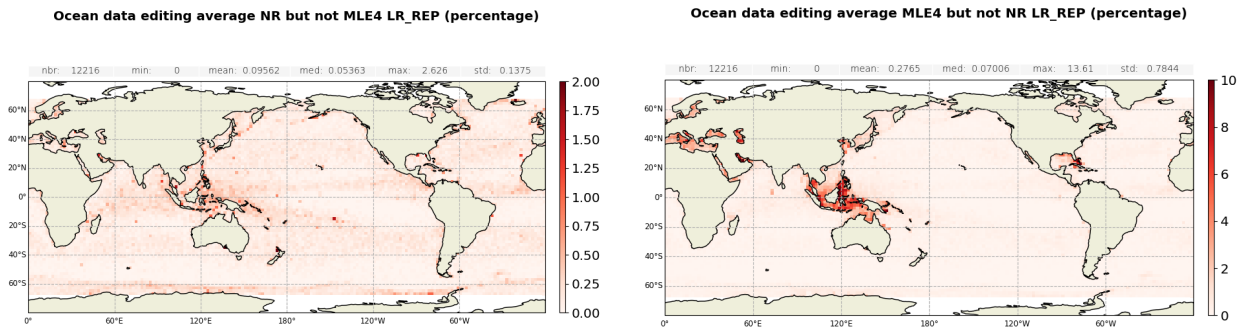

*Figure 7 – Maps of edited reprocessed measurements in NR that are valid in MLE4 (**left**) and in MLE4 that are valid in NR (**right**). The color scales are set to different widths for visibility purposes.*

4 Geophysical parameters

4.1. Altimeter parameters

Parameters derived from POS-4 altimeter are monitored in this section.

4.1.1. Significant Wave Height

4.1.1.1. LR

The time monitoring of LR Ku-band Significant Wave Height (SWH) over the complete reprocessing period is presented in figure 8, for operational (blue) and reprocessed (red for MLE4 and green for NR) datasets. As expected, no differences are observed on MLE4 with the reprocessing. Similar temporal evolutions are observed for SWH NR and MLE4. The standard deviation of NR SWH is slightly lower than for MLE4 datasets (1.378m versus 1.391m).

Figure 8 – Time monitoring of Sentinel-6 MF LR Ku-band Significant Wave Height in meters, before reprocessing (blue) and after reprocessing (red for MLE4, green for NR). Left: mean per day, Right: standard deviation per day.

The distributions of Sentinel-6 MF and Jason-3 SWH datasets are presented on figure 9. Distributions for both Sentinel-6 MF MLE4 SWH are identical and centred around 2.688m: evolutions brought by PB F07 and F08 does not impact MLE4 SWH. NR SWH is centred around a value 2.2cm higher, at 2.710m. This is in part a consequence of the anomaly in the negative NR wave management (AR 2620, see section 2.1.), which can also be seen at the low end of the distributions (right panel), where NR and MLE4 curves are not aligned up to 1.2m. Furthermore, there is no valid NR SWH below 17cm, while MLE4 SWH extend all the way to 0. Note that negative waves are edited and not considered in this analysis.
The peak in Jason-3 distribution is due to its management of low SWH. In Jason-3 processing, all 20 Hz SWH below 25 cm are set to 25 cm.

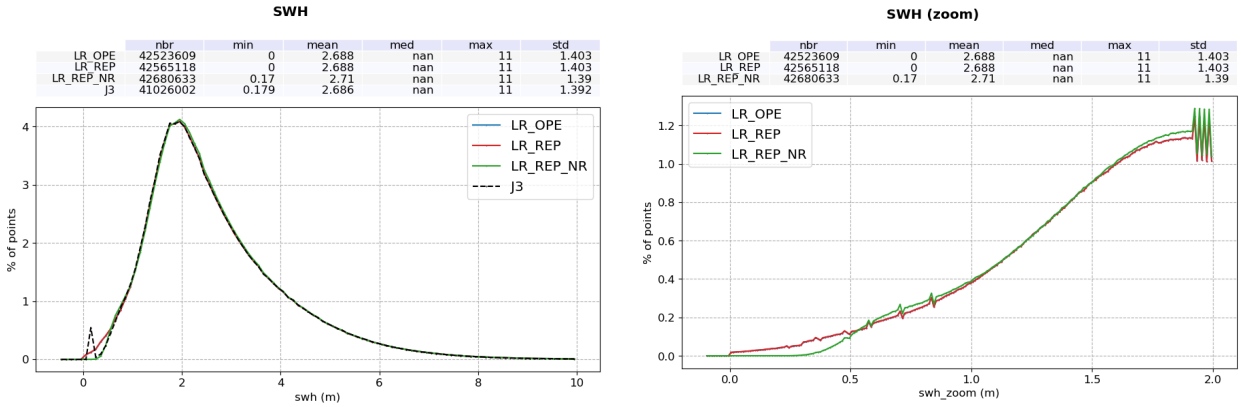

Figure 9 – Distributions of Sentinel-6 MF (blue for operational MLE4, red for reprocessed MLE4, green for NR) and Jason-3 (black) Ku-band Significant Wave Height. ***Left*** *: entire distribution,* ***right*** *: zoom without Jason-3 in the 0-2m range.*

The impact of NR SWH anomaly is also visible in figure 10, which presents the NR - MLE4 SWH difference monitoring (left panel) map (right panel), and dependency to ERA5 model SWH (bottom panel). Most differences are located in small SWH areas. The bias at very low SWH is up to 28cm, and is still about 7cm at 1m-SWH. At higher SWH, a residual bias of about 2cm remains, which can not be attributed to negative wave management, as it is unlikely to have an impact beyond the 2-3m-wave range. On the daily monitoring, a seasonal cycle is visible, as well as what could be a small drift on side B with a decrease of about 8mm in total. Such a drift would be in line with Sentinel-6 PTR ageing and would indicate an improvement brought by the numerical retracking.
This assessment will be repeated on data produced with F08 patched version in order to truly quantify the residual differences between LR MLE4 and LR NR waves.

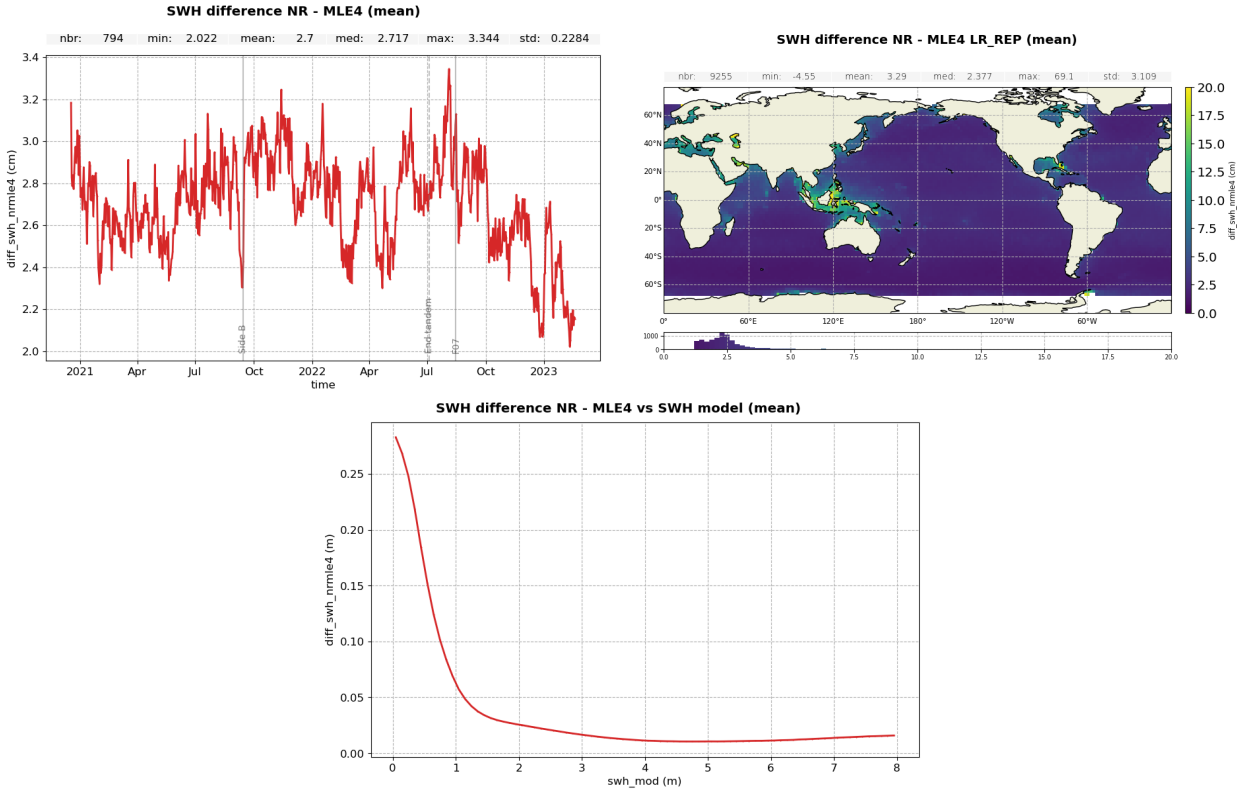

*Figure 10 – Map (**right**) and monitoring (**left**) of the LR reprocessed NR - MLE4 SWH difference in m/s per day. **Bottom** : Mean differences as a function of ERA 5 model SWH.*

To estimate the noise of 1-second along-track average of the LR Ku-band altimeter swh, we analyse "data_01/ku/swh_ocean_rms" variable from LR products. It contains the standard deviation of 20 Hz measurements used for the compression to 1hz. To retrieve 1 Hz level of noise, this value is divided by $\sqrt{20}$. Figure 11 presents the mean 1Hz SWH noise, as a function of time (left panel) and ERA 5 model SWH (right panel). The NR 1Hz SWH noise is lower than for MLE4 (which are both in line) by about 0.5cm. However, all this improvement comes from low SWH, and therefore is not representative of nominal NR performance. Beyond 3m-SWH, NR and MLE4 level of noise are in line.

4.1.1.2. HR

HR SWH monitoring highlight a small (5.6 mm) and stable difference between operational and reprocessed data (figure 12), correlated to SWH with up to 1cm bias at high SWH. This is expected and is linked to the antenna aperture update in PB F08.

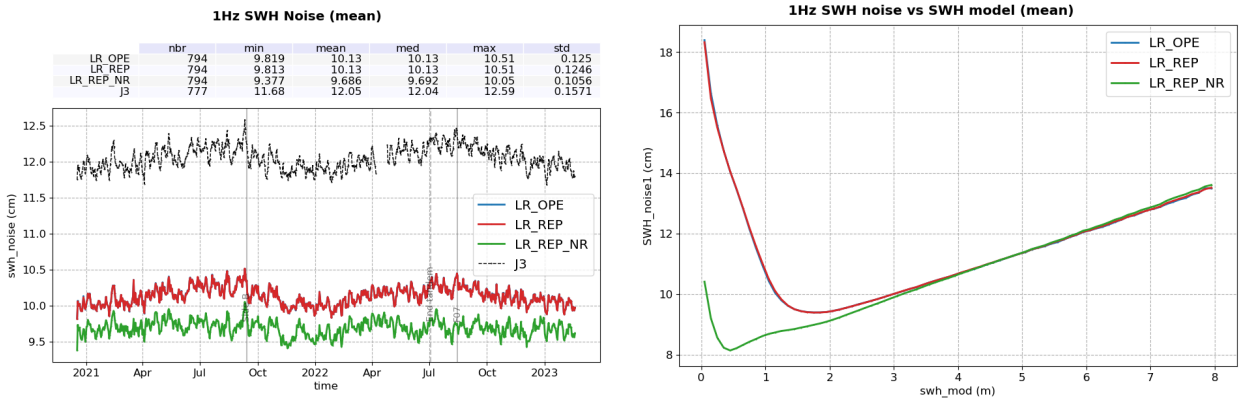

*Figure 11 – 1Hz noise for LR operational (blue) and reprocessed (red for MLE4, green for NR) SWH, as a function of time (**left**) and ERA 5 model SWH (**right**).*

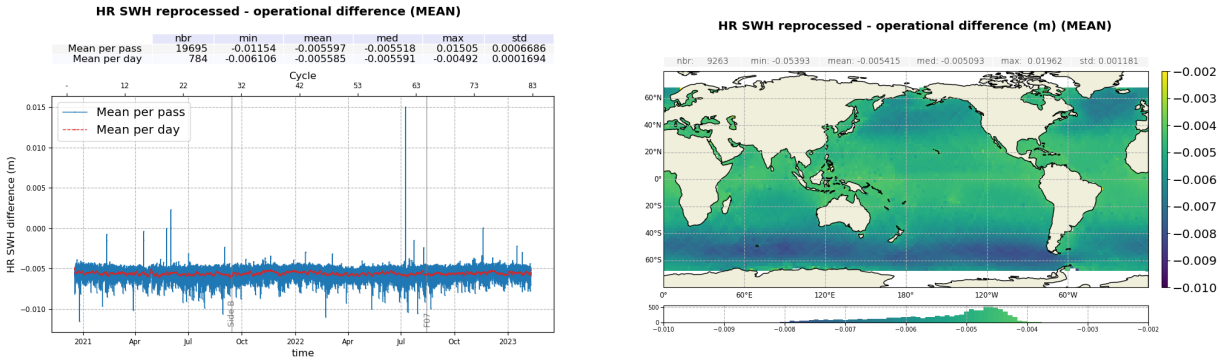

*Figure 12 – Monitoring (**left**) per day (red) and pass (blue) and map (**right**) of the reprocessed - operational HR SWH difference.*

4.1.1.3. HR-LR

The monitoring of SWH difference between HR and LR MLE4 data (figure 13) shows a small (about 5mm) reduction of the bias between the two retrievals thanks to PB F08 on the antenna aperture update impact on HR data (see previous paragraph). It is now centred around 22.7 cm with no drift between LR and HR SWH. The dependency to ERA 5 model SWH is also marginally reduced (figure 13, right panel). This bias and dependency with SWH come from the impact of the orbital wave effect which is not yet compensated on HR side.

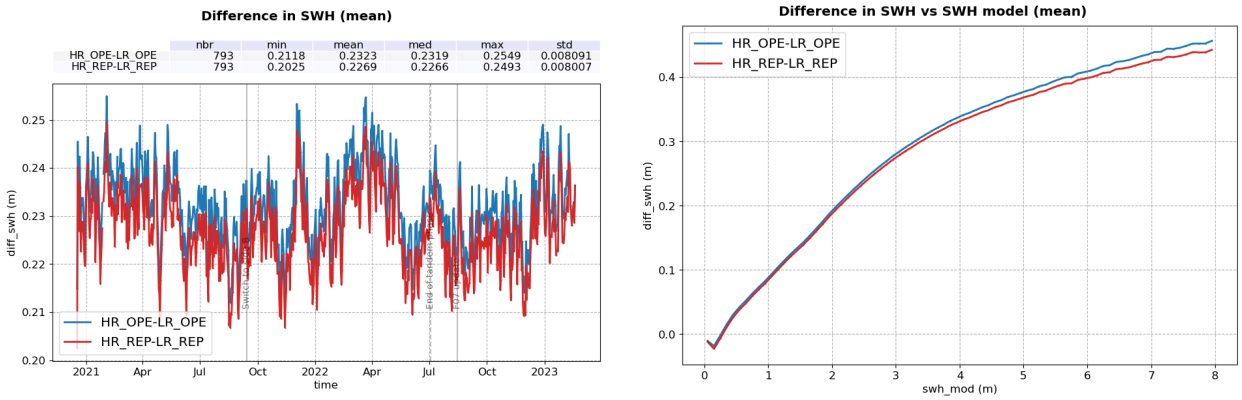

*Figure 13 – Time monitoring (**left**) and ERA 5 model SWH dependency (**right**) of Sentinel-6 MF Ku-band SWH difference : HR - LR, before reprocessing (blue) and after reprocessing (red)*

4.1.1.4. LR C-band

Figure 14 presents the time series of the reprocessed - operational LR C-band SWH and the corresponding map. No significant difference is visible.

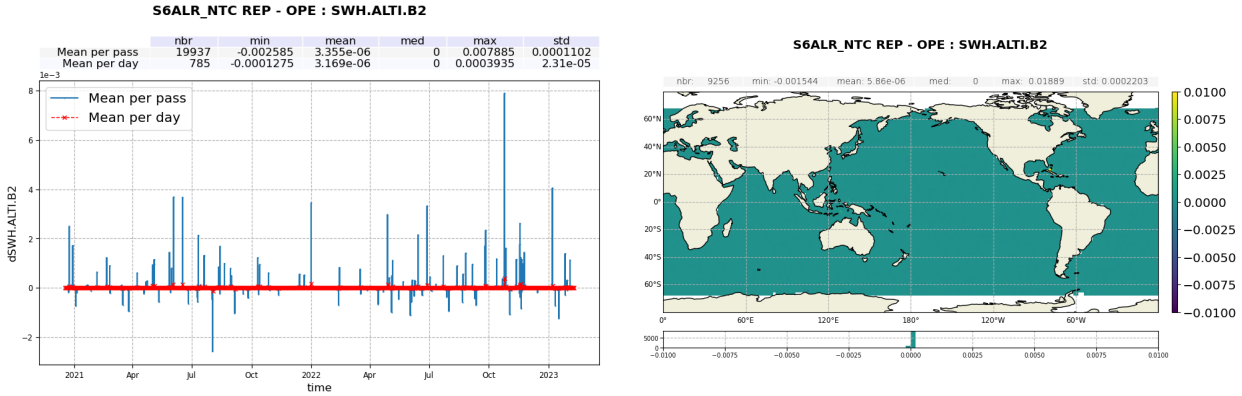

*Figure 14 – Monitoring (**left**) per day (red) and pass (blue) and map (**right**) of the reprocessed - operational C-band SWH difference.*

4.1.2. Range

4.1.2.1. LR

MLE4 operational versus reprocessed

The daily monitoring of LR MLE4 operational - reprocessed range difference is presented on figure 15 for Ku-band. Differences are submillimetric, with a small (about 0.2mm) jump at the POS4 side B switch on 2021-09-14, and a change of behaviour from F07 update on 2022-08-15, with only negligible differences afterward. This last change might be linked to the ECHO CAL update implemented in PB F07.

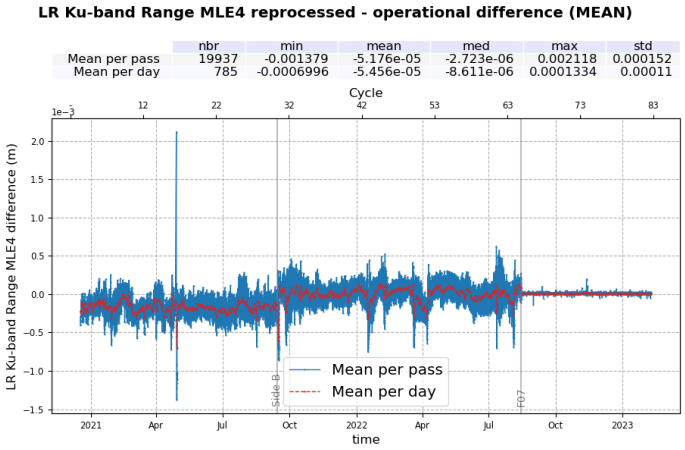

Figure 15 – Monitoring of the LR MLE4 operational - reprocessed range difference per day (red) and per pass (blue) for Ku-band.

Reprocessed MLE4 versus NR

The daily monitoring of LR reprocessed NR - MLE4 range difference is presented on figure 16. A -1mm jump on the mean (left panel) is visible at the side B switch on 2021-09-14. The main hypothesis for this jump is this instrumental LUT applied on MLE4 range, which is for the moment identical for both POS4-A and POS4-B. The standard deviation monitoring (right panel) presents a yearly variation with higher values from June to September and lower values from December to May, and can be linked with seasonal SWH variations (cf below).
The NR - MLE4 range distributions are presented on figure 17 for side A (left panel) and side B (right panel). Ranges are consistent between both retrackings, with only a 6.7mm bias on side A and 5.7mm on side B.

On figure 18 is presented the map of the F08 NR - MLE4 range difference (left panel) and its dependency to ERA 5 model SWH (right panel). The differences are correlated to SWH, with a decrease of about -6mm between 0 and 0.5m-SWH and then about +7.5mm increase between 0.5 and 7m SWH. This bias increase is expected and caused by the MLE4 LUT.

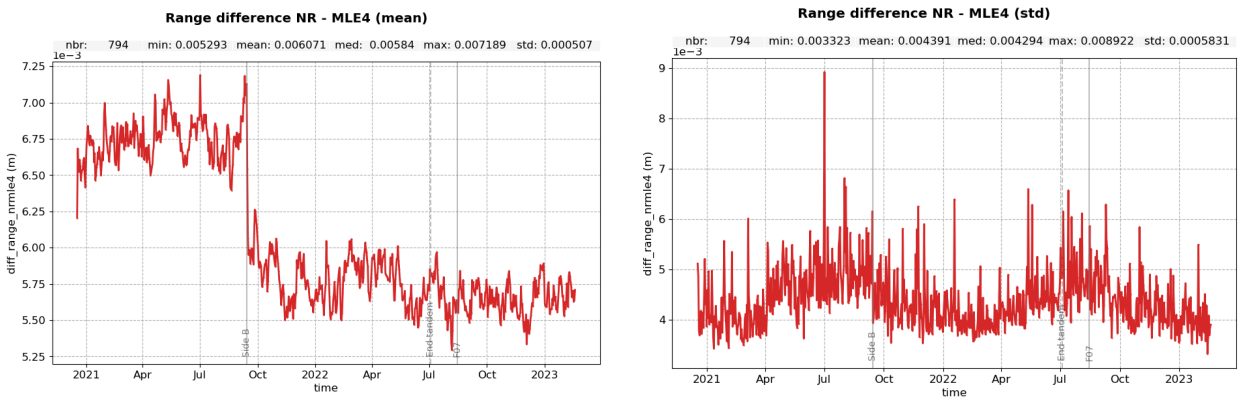

*Figure 16 – Time monitoring of Sentinel-6 MF F08 NR - MLE4 range difference per day, for the mean (**left**) and the standard deviation (**right**).*

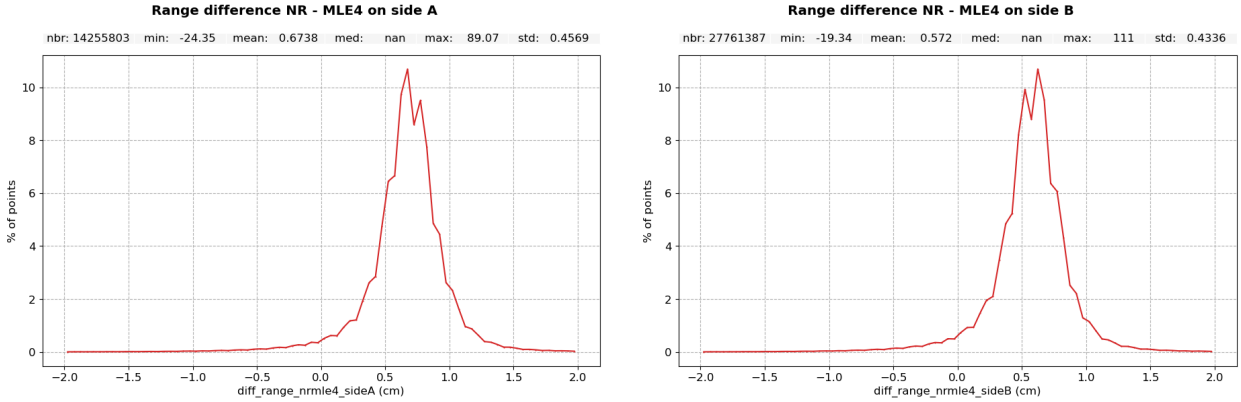

*Figure 17 – Distributions of Sentinel-6 MF F08 NR - MLE4 range difference for side A (**left**) and side B (**right**).*

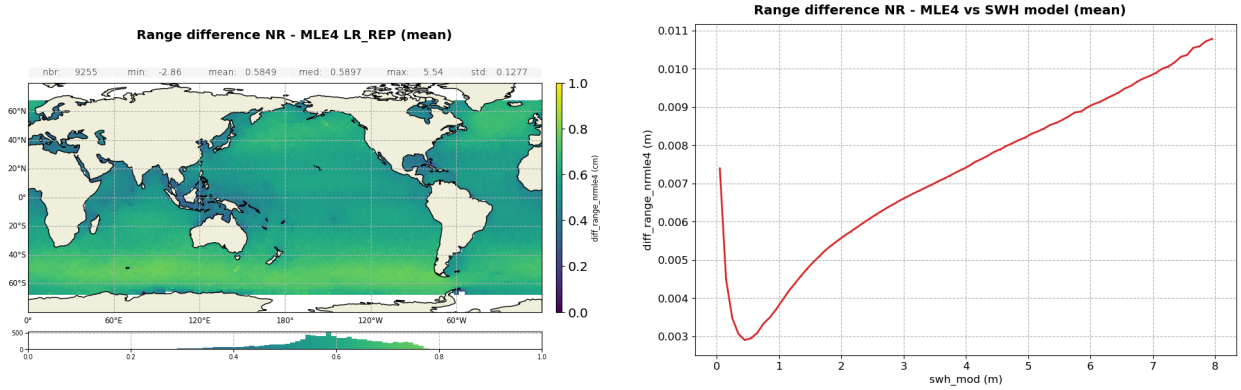

*Figure 18 – Map (**left**) and ERA 5 model SWH dependency (**right**) of the LR F08 NR - MLE4 range difference.*

4.1.2.2. HR

The daily monitoring of HR operational - reprocessed range difference is presented on figure 19, left panel. Differences are submillimetric, with a bias of about 0.5mm stable in time after a small (about 0.2mm) jump at the POS4 side B switch on 2021-09-14. The map of these differences (right panel) shows SWH-dependent regional differences. This is expected and linked to the antenna aperture update.

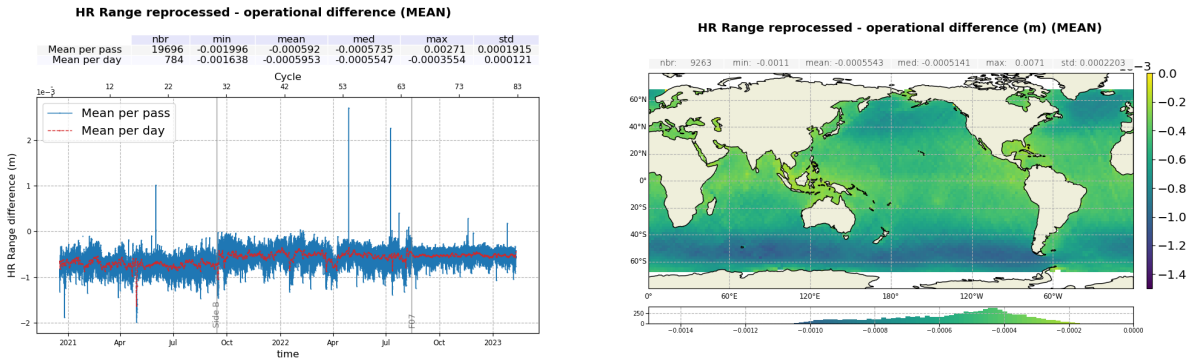

*Figure 19 – Map (**right**) and monitoring (**left**) of the HR operational - reprocessed range difference per day (red) and per pass (blue).*

4.1.2.3. HR - LR

HR versus LR MLE4 range bias is monitored in figure 20. Using MLE4 range, the bias is reduced by about 0.5mm with the reprocessing thanks to HR as seen in the previous paragraph (1.87cm versus 1.92cm in operational data). A drift of -1mm/year is seen in both MLE4 datasets, and can be linked to the PTR deformation. Using LR NR, the bias reduction is much more significant, at only 1.26cm, and the use of the in-flight LR PTR shape reduces the drift between LR and HR to -0.3mm/year.
A marginal decrease in SWH correlation (right panel) is observed with the reprocessing in MLE4. This SWH dependency comes from the usage of a skewness coefficient of 0 on HR side whereas the it is set to 0.1 on LR side.

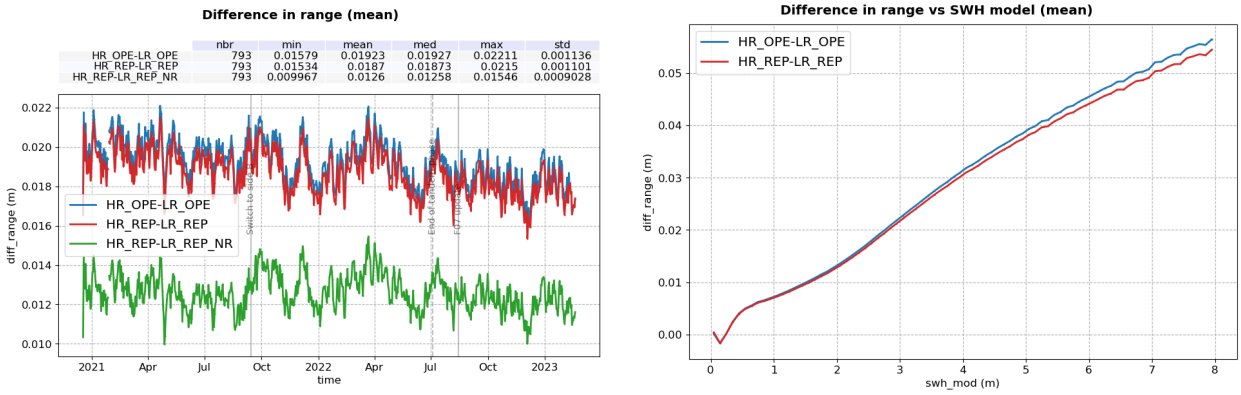

*Figure 20 – Time monitoring (**left**) and ERA 5 model SWH dependency (**right**) of Sentinel-6 MF Ku-band Range difference : HR - LR, before reprocessing (blue) and after reprocessing (red with LR MLE4 and green for LR NR)*

Along track wind has a known impact on HR data and more particularly on HR range [8]. To highlight this impact, two gridded maps of HR versus LR range difference are drawn, one for ascending tracks and the other one for descending tracks. Next, the difference between these two maps is computed (ascending minus descending). Such process allows to remove all systematic error on the bias (such as waves) and to only highlight HR variations with respect to LR that depend on track orientation.
Figure 21 shows the resulting maps for both operational and reprocessed data. No significant difference can be seen between the two datasets.

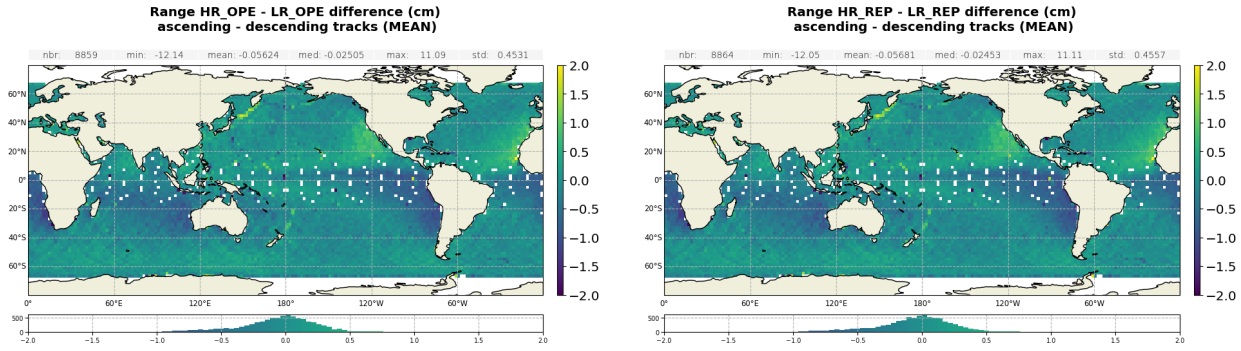

Figure 21 – Maps of Ascending versus Descending tracks maps of HR versus LR MLE4 range bias. Left panel: for operational data. Right panel: for reprocessed data.

4.1.2.4. LR C-band

Figure 22 presents the time series of the reprocessed - operational LR C-band range and the corresponding map. No significant difference is visible.

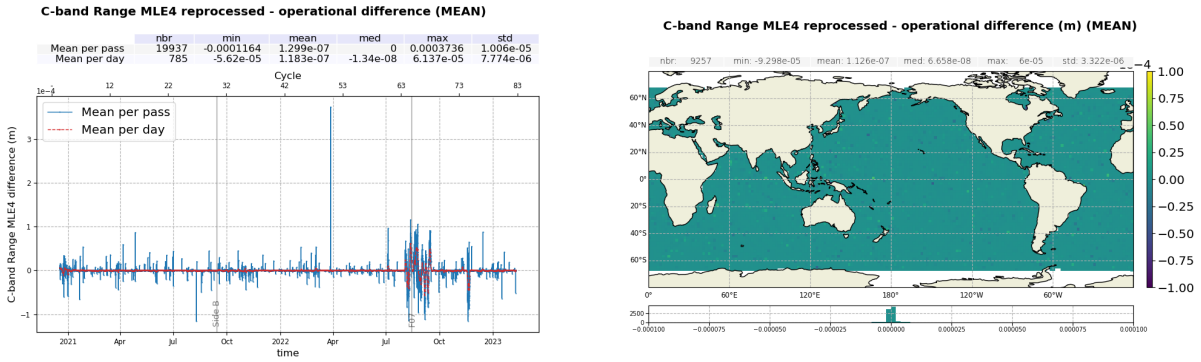

*Figure 22 – Monitoring (**left**) per day (red) and pass (blue) and map (**right**) of the reprocessed - operational C-band range difference.*

4.1.3. Backscatter coefficient

4.1.3.1. LR

Ku-band backscatter coefficient (sigma0) time series are presented on figure 23 and their distributions, on figure 24. The bias between reprocessed and operational MLE4 sigma0 is of -0.09dB, and the bias between reprocessed NR and MLE4 is 0.89dB. The standard deviation is slightly higher in NR (1.61dB) than in MLE4 (1.59dB for both operational and reprocessed).

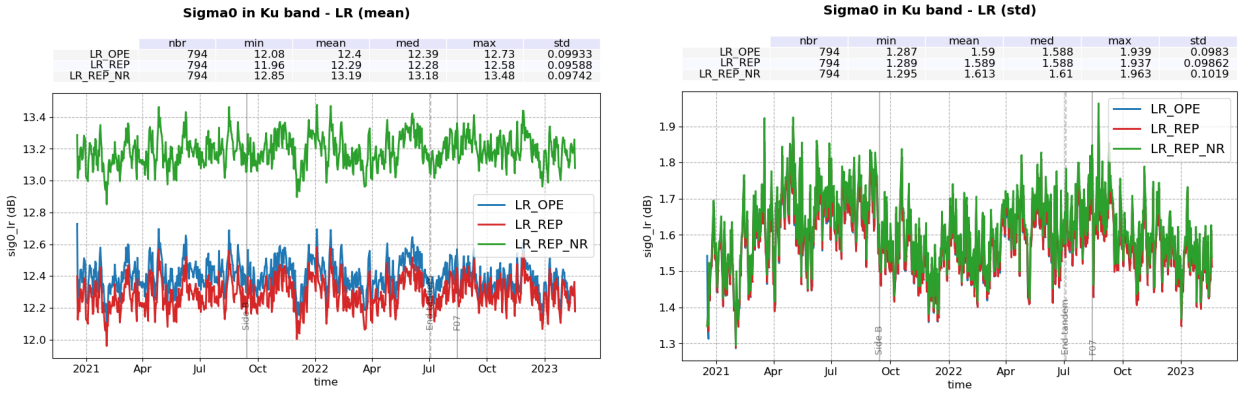

Figure 23 – Time monitoring of Sentinel-6 MF LR Ku-band Backscatter coefficient in dB, before reprocessing (blue) and after reprocessing (red for MLE4 and green for NR). Left: mean per day, Right: standard deviation per day.

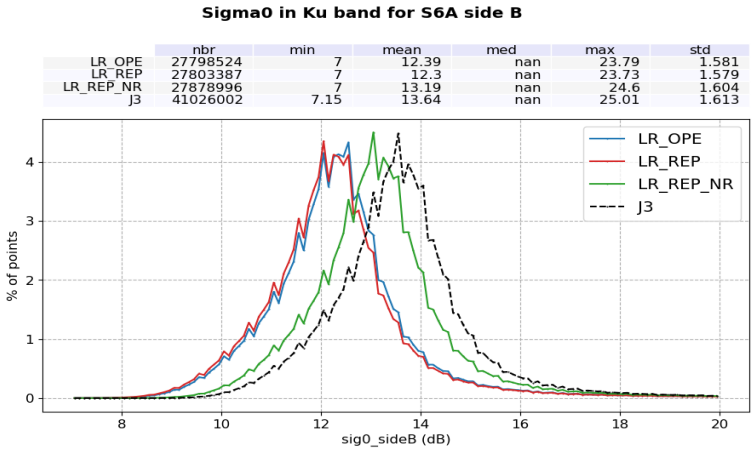

Figure 24 – Histogram of Sentinel-6 MF LR Ku-band Backscatter coefficient in dB, before reprocessing (blue) and after reprocessing (red for MLE4 and green for NR) and Jason-3 (black).

MLE4 operational versus reprocessed

Looking more closely at the differences between operational and reprocessed MLE4 sigma0 (figure 25), two jumps are visible :

- 0.02dB on 2021-09-14 at the POS-4 side B switch.
- 0.06dB on 2022-08-15 at the PB F07 update. This is linked to the ECHO CAL becoming the main source for CAL 1.

After this last jump, the remaining bias is close to -0.06dB and is linked to the PB F08 antenna aperture update. Note that the radiometer calibration anomaly from October to December 2022 (see section 4.2.) is also visible with a very small amplitude. It is due to use of the atmospheric attenuation, derived for the radiometer, in the computation of the sigma0.
On the corresponding map on the right panel of figure 25, we note the existence of low amplitude regional patches and much lower differences in the Caspian Sea. This Caspian Sea discrepancy is explained by the fact that only data simultaneously valid in both datasets were kept. Indeed, before the PB F07 update, no filtered ionospheric correction was available on the Caspian Sea and the data was edited. Therefore, this area only contains data from the 0.06dB F07/F08 bias distribution.

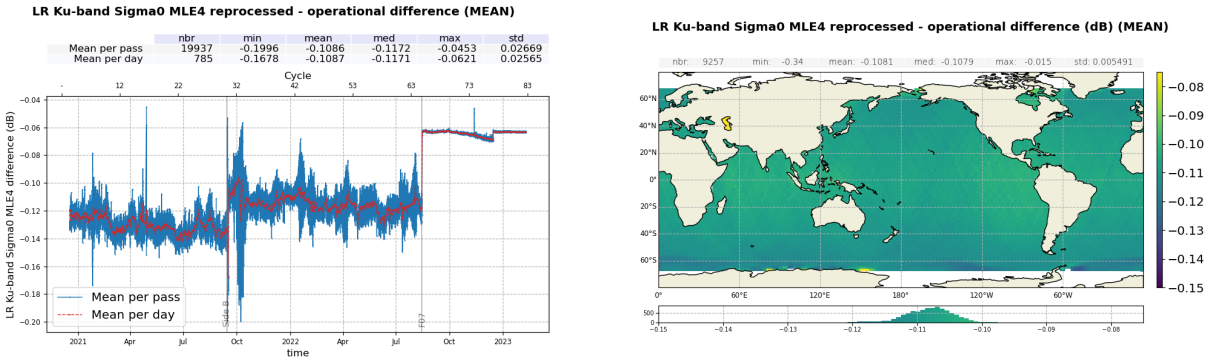

*Figure 25 – Map (**right**) and monitoring (**left**) of the LR MLE4 operational - reprocessed sigma0 difference per day (red) and per pass (blue).*

Reprocessed MLE4 versus NR

Figure 26 presents the sigma0 differences between reprocessed NR and MLE4. On the time series, a drift of very small amplitude can be observed (+0.003dB on the entire side B). This drift is still monitored and is under investigation.
In the corresponding map (right panel), the sigma0 difference is slightly correlated with high Mean Sea Surface (MSS) gradients, which corresponds to sudden changes in bathymetry. This indicates that both retrackers have different sensitivities to sea surface slopes, however the exact explanation is not yet understood. Additionally, the bias on the Caspian Sea is significantly lower than on ocean. LR NR is not affected by the sampling ratio anomaly in the computation of the total power since it uses the peak power of the PTR.

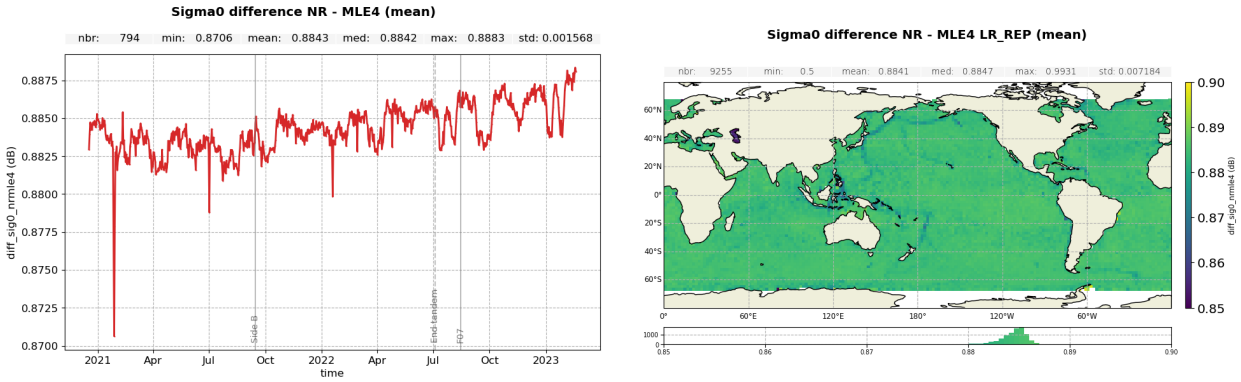

*Figure 26 – Map (**right**) and monitoring (**left**) of the LR reprocessed NR - MLE4 sigma0 difference per day.*

4.1.3.2. HR

The HR reprocessed - operational Ku-band backscatter coefficient difference present the same features as in LR MLE4 (figure 27). While jumps at the side B switch and PB F07 update have amplitudes identical to LR, the remaining F07/F08 bias due to the antenna aperture update is of only -0.01dB.

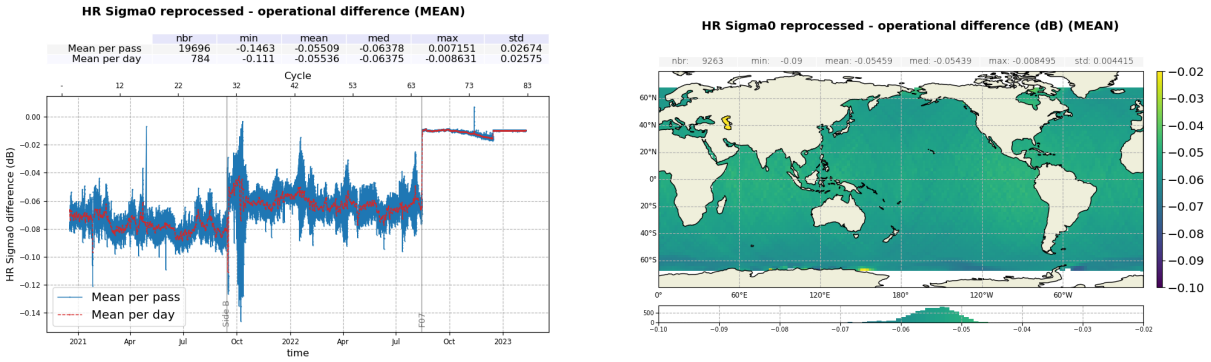

*Figure 27 – Map (**right**) and monitoring (**left**) of the HR operational - reprocessed sigma0 difference per day (red) and per pass (blue).*

4.1.3.3. HR - LR

HR versus LR MLE4 sigma0 bias is monitored in figure 28. The bias increased from 5.46 to 5.63dB with the reprocessing. This was expected because of the antenna aperture update impacting differently LR and HR (see previous paragraphs). Otherwise, there is no significant evolution.

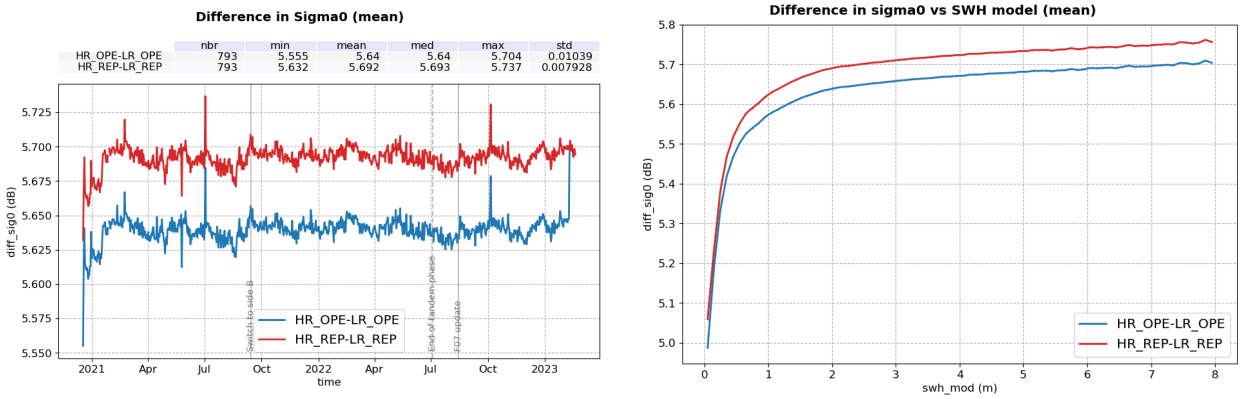

*Figure 28 – Time monitoring (**left**) and ERA 5 model SWH dependency (**right**) of Sentinel-6 MF Ku-band sigma0 difference : HR - LR MLE4, before reprocessing (blue) and after reprocessing (red with LR MLE4)*

4.1.3.4. LR C-band

Figure 29 presents the time series of the reprocessed - operational LR C-band sigma0 and the corresponding map. As in Ku-band, the corrected WTC drift from October to December 2021, due to use of the atmospheric attenuation in the computation of the sigma0, is visible. No other significant difference is visible.

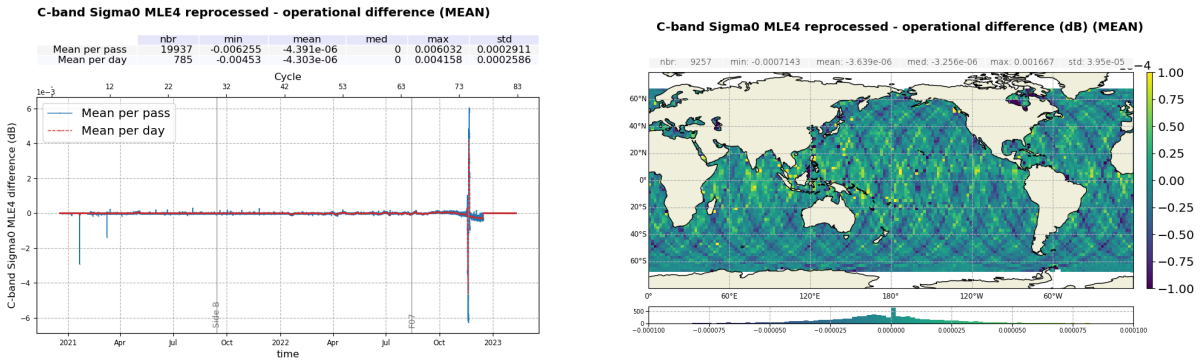

*Figure 29 – Monitoring (**left**) per day (red) and pass (blue) and map (**right**) of the reprocessed - operational C-band sigma0 difference.*

4.1.4. Altimeter Wind Speed

4.1.4.1. LR

As for the backscatter coefficient, operational and reprocessed LR altimeter wind speeds are in line from PB F07 (figure 30, left panel). The standard deviation average across the entire time series (right panel) slightly increased after the reprocessing (3.76m/s for MLE4 and 3.78m/s for NR) compared to operational data (3.72 m/s). After reprocessing, LR wind-speed is centred around 8.32m/s for MLE4 and 8.31m/s for NR, which is higher than for operational data (8.17m/s) and Jason-3 (8.14m/s).

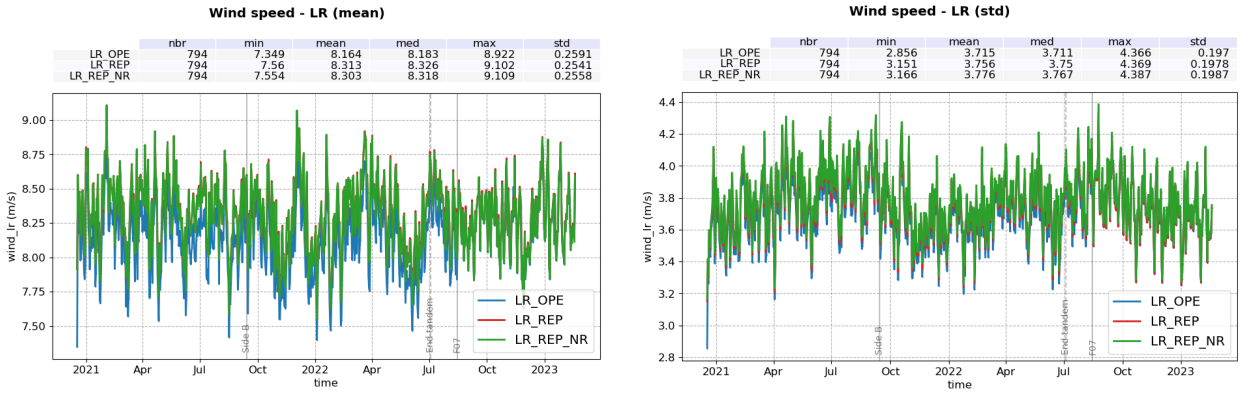

*Figure 30 – Time monitoring of Sentinel-6 MF altimeter wind-speed in m/s, before reprocessing (blue) and after reprocessing (red for MLE4, green for NR). **Left**: mean per day, **Right**: standard deviation per day.*

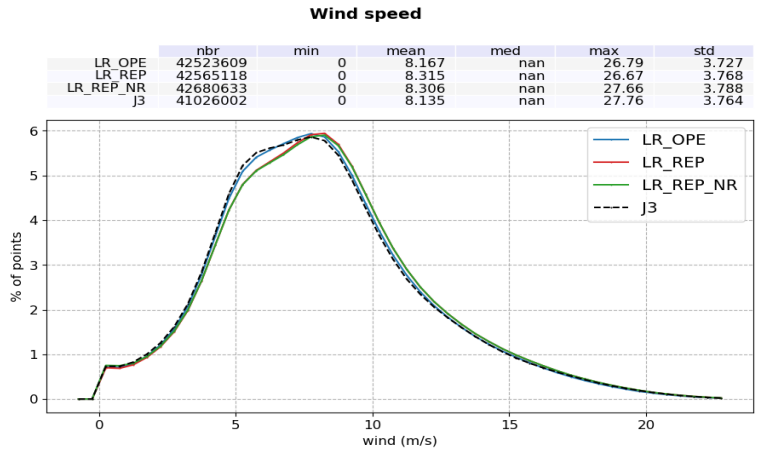

Figure 31 – Histogram of altimeter wind-speed for Jason-3 (black), reprocessed S6 MF LR (blue) and reprocessed S6 MF HR (red). Computed over the completed reprocessed period.

MLE4 operational versus reprocessed

Looking more closely to the reprocessed - operational differences (figure 32), a small jump is visible at the side B switch (2021-09-14), as well as a 20cm/s jump at the PB F07 update. This behavior is consistent with what is seen on the backscatter coefficient (see section 4.1.3.) and was therefore expected. The map (right panel) shows a correlation with wind speed, with regional differences ranging from about 7 to 20 cm/s.

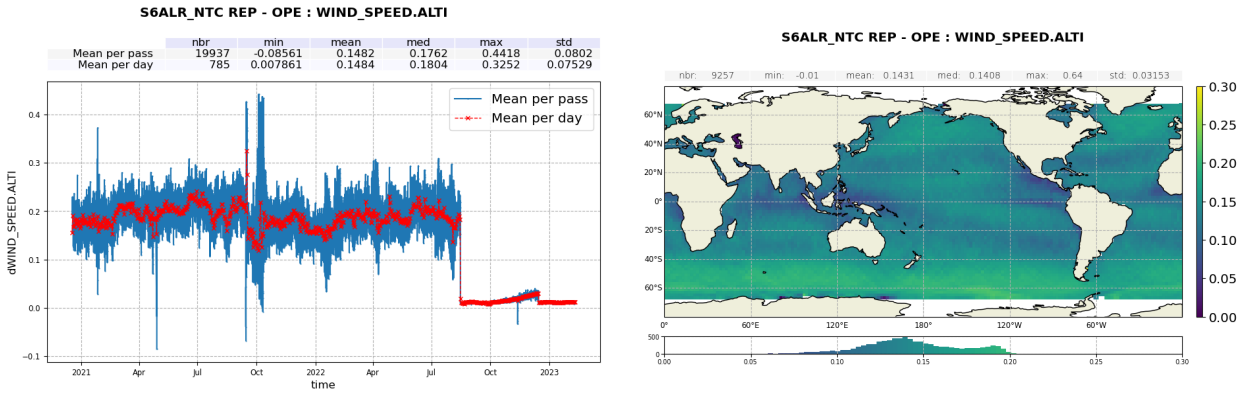

*Figure 32 – Map (**right**) and monitoring (**left**) of the LR MLE4 operational - reprocessed wind speed difference per day (red) and per pass (blue).*

Reprocessed MLE4 versus NR

Figure 33 presents the wind speed differences between reprocessed NR and MLE4. On the time series, as for the sigma0, a drift of very small amplitude can be observed (-1cm/s on the entire side B). This drift is still monitored and is under investigation.
Unsurprisingly, the corresponding map (right panel) presents similar features to the NR - MLE4 sigma0 differences map presented on figure 26, with a correlation with high Mean Sea Surface (MSS) gradients and a different bias on the Caspian Sea.
The differences are correlated to the SWH (bottom panel), with a +5cm/s increase between 0.5 and 8m-SWH.

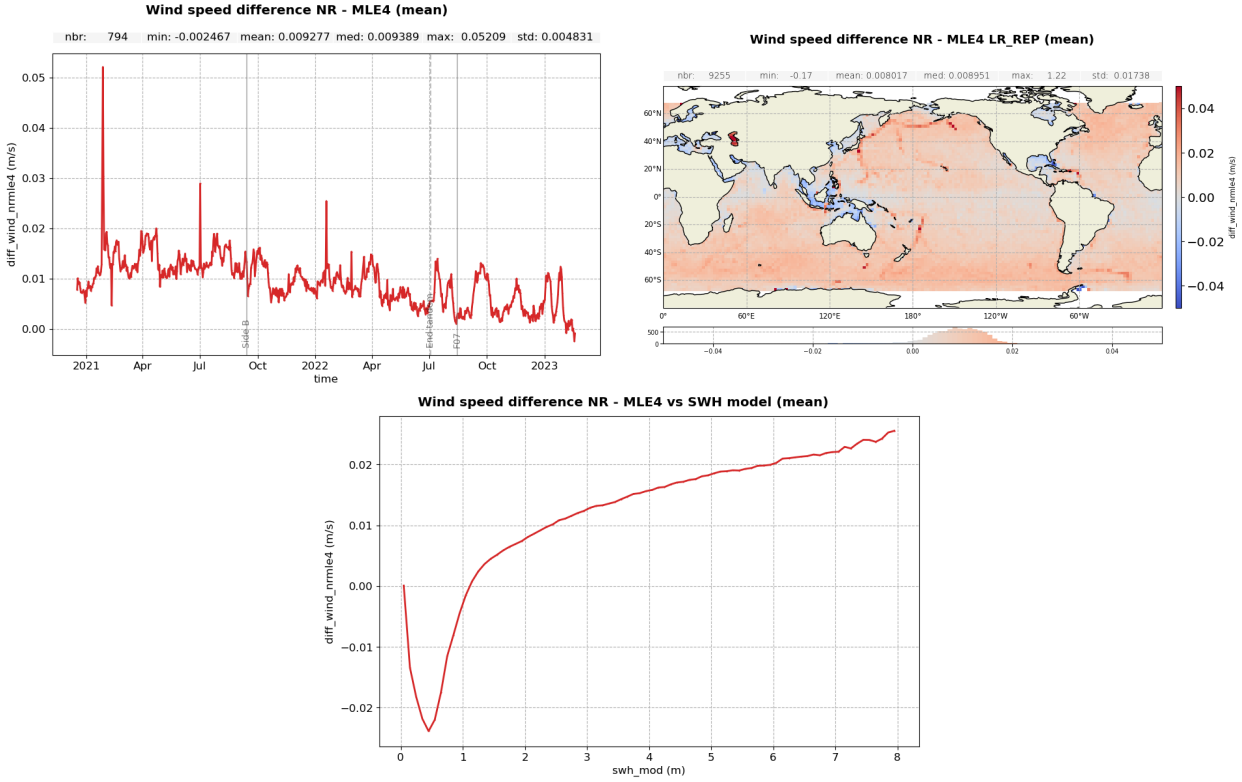

*Figure 33 – Map (**right**) and monitoring (**left**) of the LR reprocessed NR - MLE4 wind speed difference in m/s per day. **Bottom** : Mean differences as a function of ERA 5 model SWH.*

Comparison to ECMWF model

The daily monitoring of the comparison of altimeter-derived wind speed to ECMWF model is presented on figure 34. Both reprocessed datasets are aligned, with a mean bias of 35.1cm/s in MLE4 and 35.6cm/s in NR, stable on side B and slightly decreasing on side A starting from April 2021 with peaks above 60cm/s. As expected from previous paragraphs, the mean of the operational dataset is almost aligned with the reprocessed datasets after the PB F07 update. Standard deviation is slightly higher for NR (1.47m/s) compared to MLE4 (1.45m/s and 1.46m/s for operational and reprocessed respectively), and presents small seasonal variations.

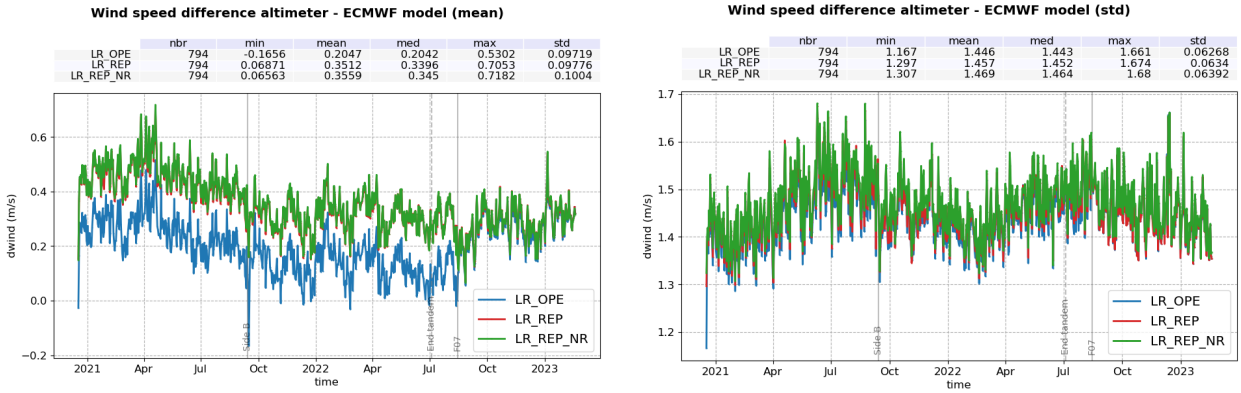

*Figure 34 – Time monitoring of Sentinel-6 MF altimeter - ECMWF model wind speed difference in m/s, before reprocessing (blue) and after reprocessing (red for MLE4, green for NR). **Left**: mean per day, **Right**: standard deviation per day.*

4.1.4.2. HR

The HR reprocessed - operational wind speed difference present the same features as in LR MLE4 (figure 35). There is no significant difference after the PB F07 update except for the corrected impact of the radiometer drift from October to December 2021.

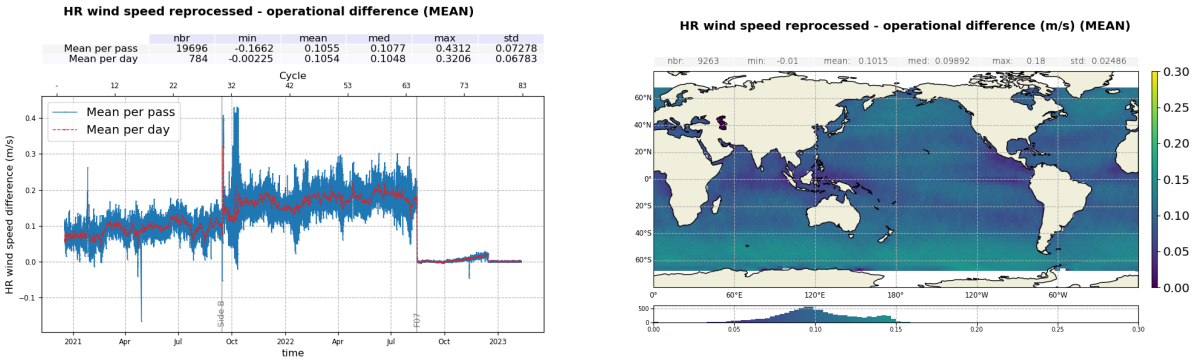

*Figure 35 – Map (**right**) and monitoring (**left**) of the HR operational - reprocessed wind speed difference per day (red) and per pass (blue).*

4.1.4.3. HR - LR

HR versus LR MLE4 wind speed bias is monitored in figure 36. An unexpected jump of about 10cm/s is visible at the side B switch on the reprocessed dataset. In order to identify its origin, the sigma0 bias with Jason-3 during the tandem phase will be quantified for all reprocessed LR and HR datasets. This will be presented on the next version of this report.

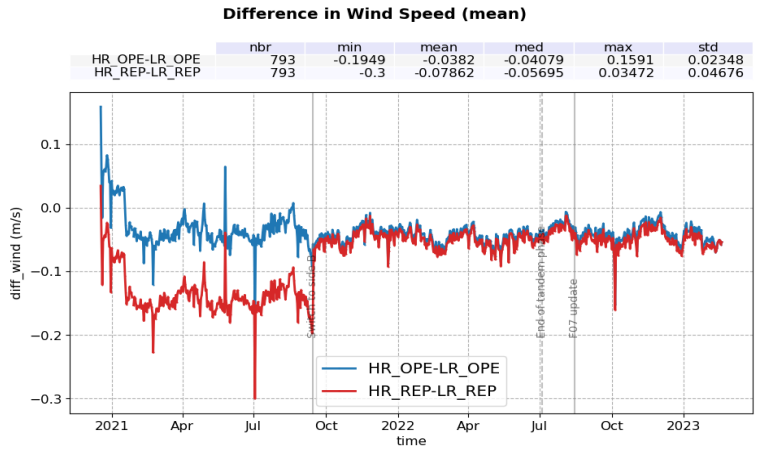

Figure 36 – Time monitoring of Sentinel-6 MF wind speed difference : HR - LR MLE4, before reprocessing (blue) and after reprocessing (red with LR MLE4) per day.

4.1.5. Sea State Bias

4.1.5.1. LR

SSB time series are presented on figure 37 and their distributions, on figure 38. Biases are submillimetric and all datasets follow identical variations.

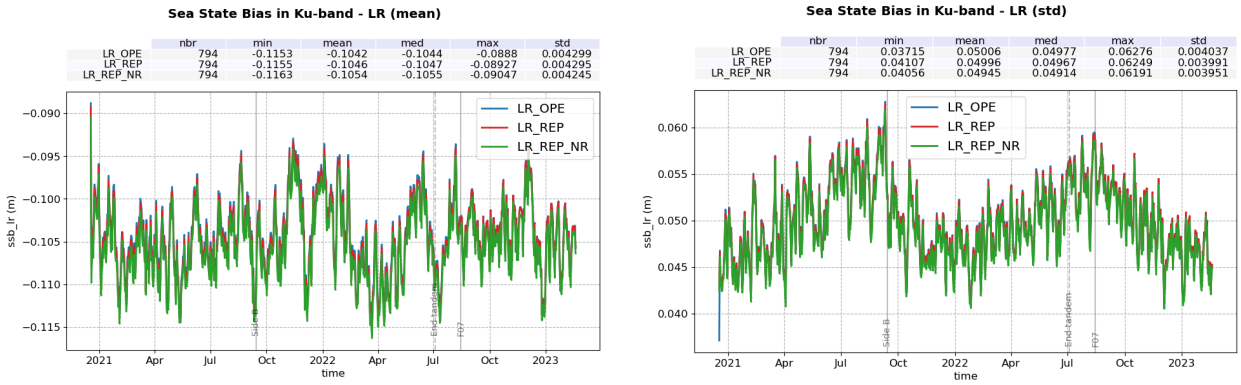

Figure 37 – Time monitoring of Sentinel-6 MF LR SSB in meters, before reprocessing (blue) and after reprocessing (red for MLE4 and green for NR). Left: mean per day, Right: standard deviation per day.

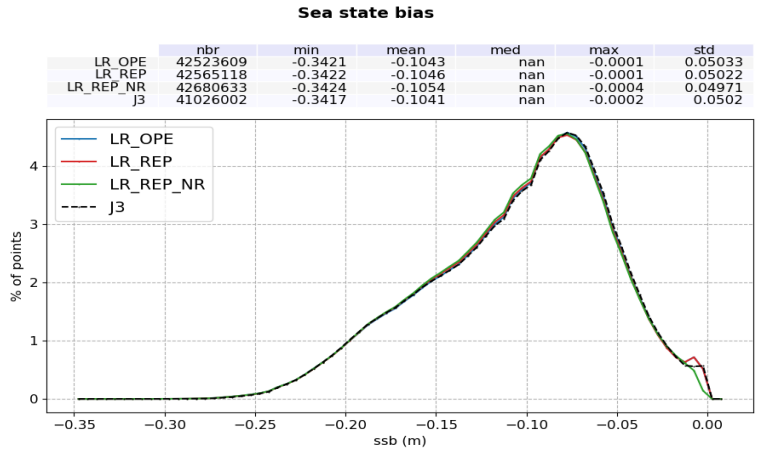

Figure 38 – Histogram of Sentinel-6 MF LR SSB in meters, before reprocessing (blue) and after reprocessing (red for MLE4 and green for NR) and Jason-3 (black).

MLE4 operational versus reprocessed

Looking more closely to the reprocessed - operational differences (figure 39), a small 0.4mm jump is visible at the PB F07 update. It is due to the wind speed evolution at the same date. The map (right panel) shows a correlation with SWH, with submillimetric regional variations.

Reprocessed MLE4 versus NR

Figure 40 presents the SSB differences between reprocessed NR and MLE4. No clear jump or drift is visible in the daily monitoring, although yearly variations with amplitudes reaching up to 0.5mm can be seen. These variations are the result of the significant SWH correlation that is visible on the corresponding map (right panel) and in the mean difference as a function of ERA 5 model SWH (bottom panel), with an almost +6mm increase between 0 an 8m-SWH.

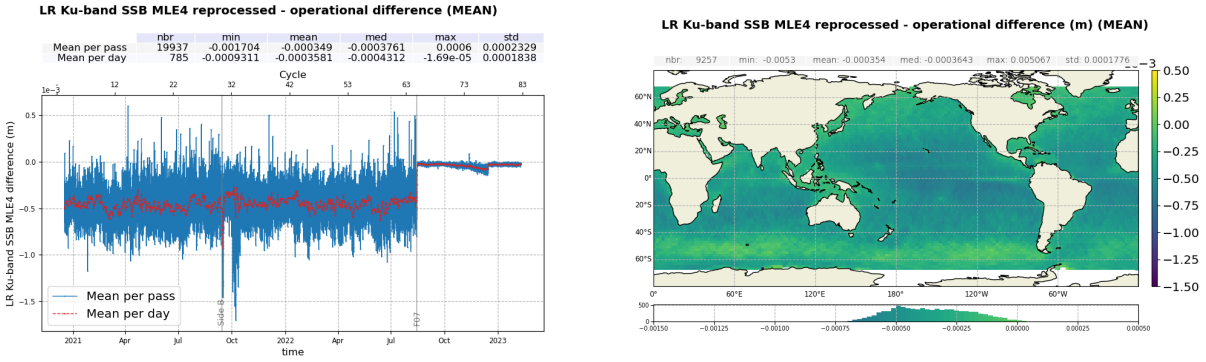

*Figure 39 – Map (**right**) and monitoring (**left**) of the LR MLE4 operational - reprocessed SSB difference per day (red) and per pass (blue).*

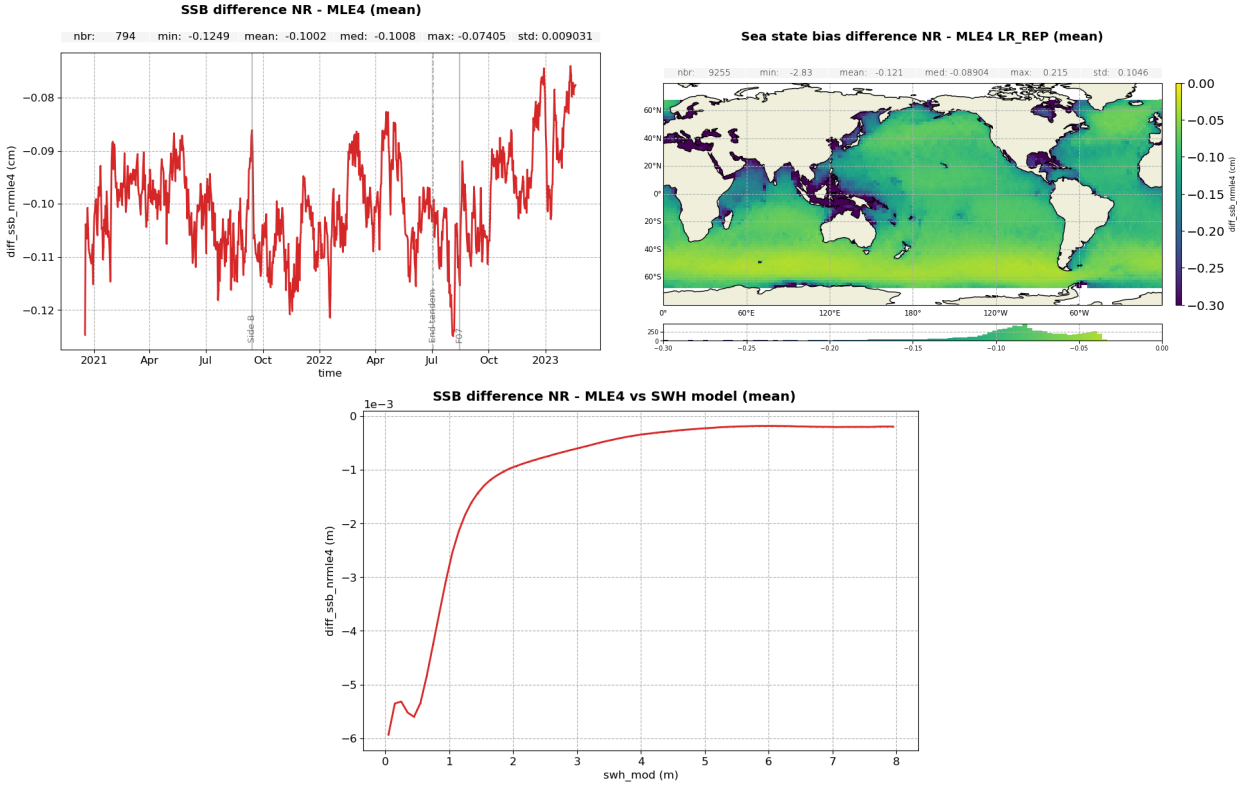

*Figure 40 – Map (**right**) and monitoring (**left**) of the LR reprocessed NR - MLE4 SSB difference per day in cm. **Bottom** : Mean differences in meters as a function of ERA 5 model SWH.*

4.1.5.2. HR

As in LR, the HR reprocessed - operational SSB difference presents a small jump at the PB F07 update of about +0.5mm (figure 41). Additionally, a change in behavior is visible between sides A and B, with a slightly more significant negative bias on side B. As in LR, the map (right panel) shows a correlation with SWH, with submillimetric regional variations.

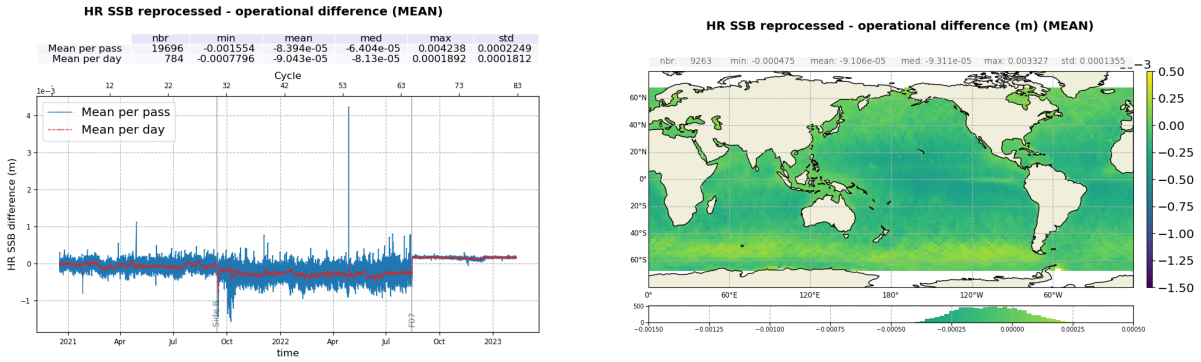

*Figure 41 – Map (**right**) and monitoring (**left**) of the HR operational - reprocessed SSB difference per day (red) and per pass (blue).*

4.1.5.3. HR - LR

HR versus LR MLE4 SSB bias is monitored in figure 42. As with the wind speed, an unexpected jump of about 0.5mm is visible at the side B switch on the reprocessed dataset. In order to identify its origin, the sigma0 bias with Jason-3 during the tandem phase will be quantified for all reprocessed LR and HR datasets. This will be presented on the next version of this report.

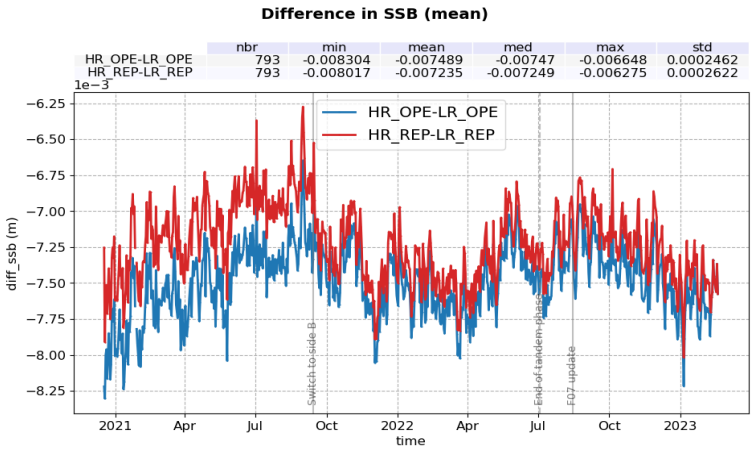

Figure 42 – Time monitoring of Sentinel-6 MF SSB difference : HR - LR MLE4, before reprocessing (blue) and after reprocessing (red with LR MLE4) per day.

4.1.5.4. LR C-band

Figure 43 presents the time series of the reprocessed - operational LR C-band SSB and the corresponding map. As in Ku-band, a small jump is visible at the PB F07 update, with an amplitude of about 0.75mm. Also similarly to Ku-band, the corresponding maps highlights a correlation to SWH with an amplitude of about 1mm.

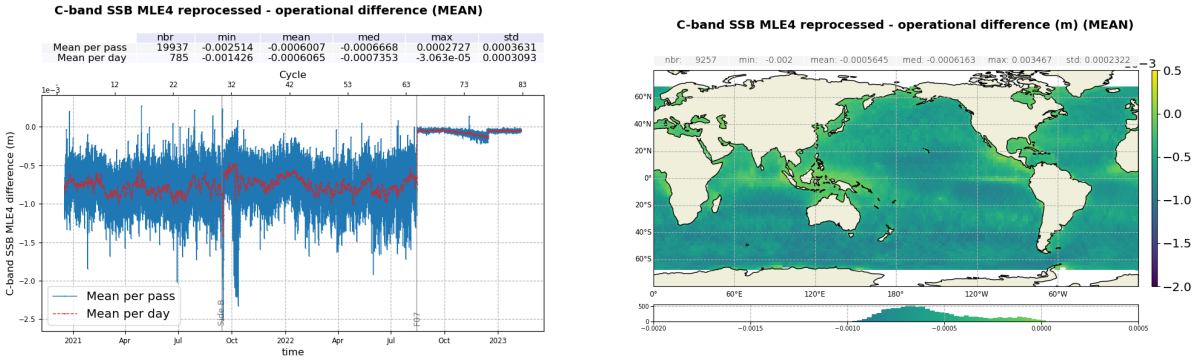

*Figure 43 – Monitoring (**left**) per day (red) and pass (blue) and map (**right**) of the reprocessed - operational C-band SSB difference.*

4.1.6. Altimeter ionosphere correction

Sentinel-6 MF altimeter ionosphere correction is derived from LR data, in Ku and C-band. The ionosphere correction in HR products is copied from LR products and thus identical. Filtered ionosphere correction from altimeter is analysed in this section.

Operational and reprocessed ionosphere corrections are in line for all datasets, both in mean and in standard deviation (figure 44). On this monitoring, a decrease of the ionosphere correction is visible. This expected behavior is due to the current increase in activity along the solar cycle.

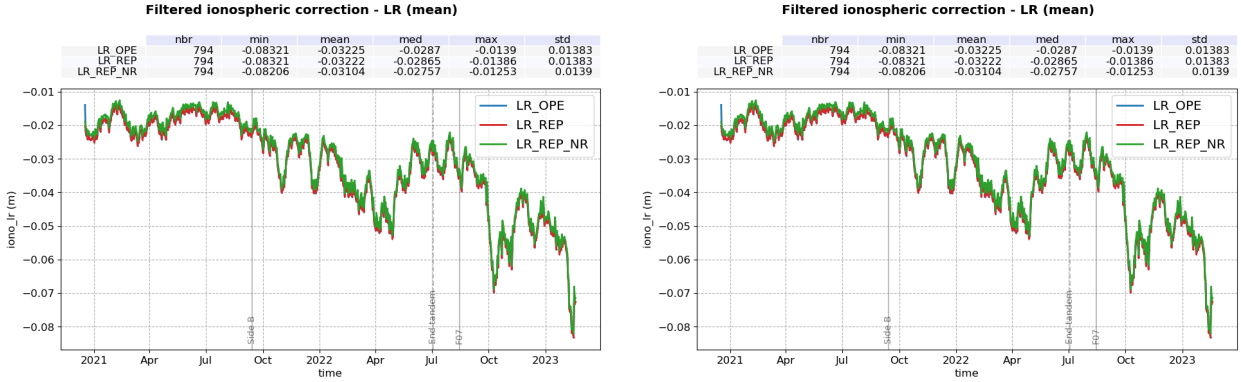

*Figure 44 – Time monitoring of Sentinel-6 MF LR Altimeter filtred ionosphere correction in meters, before reprocessing (blue) and after reprocessing (red for MLE4, green for NR). **Left**: mean per day, **Right**: standard deviation per day.*

On the histogram of the distributions (figure 45), NR ionosphere correction (-3.12cm) shows a small 1.2mm bias with respect to MLE4 (-3.24 cm in both MLE4 datasets).

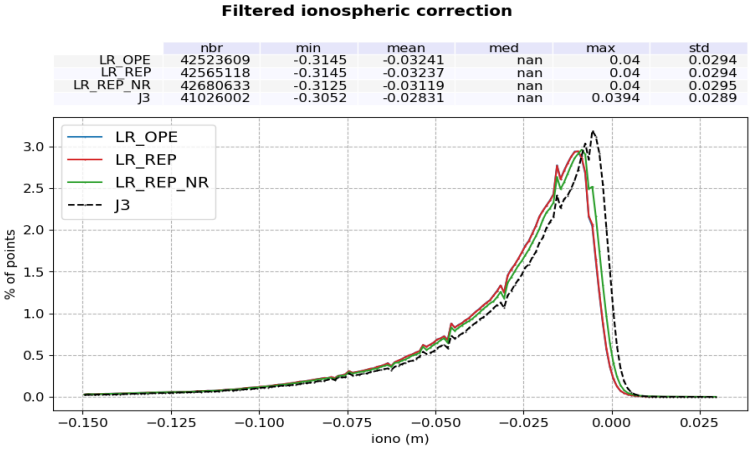

Figure 45 – Histogram of altimeter filtred ionosphere correction for Jason-3 (black) and reprocessed Sentinel-6 MF LR (blue for operation MLE4, red for reprocessed MLE4, green for reprocessed NR). Computed over the completed reprocessed period.

Figure 46 presents the daily monitoring of the NR - MLE4 filtred ionospheric correction difference. An about -0.25mm jump is visible at the side B switch.

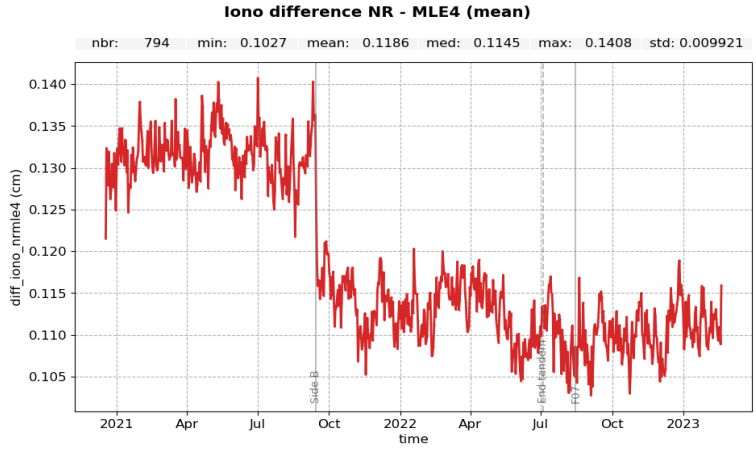

Figure 46 – Time monitoring of the NR - MLE4 filtred ionospheric correction difference per day in cm.

Reprocessed Sentinel-6 MF altimeter ionosphere corrections show in average a better consistency to GIM model than Jason-3 (figure 47, left panel), with a 9mm bias in MLE4, a 10mm bias in NR and a 13mm bias for Jason-3. However, looking at the corresponding maps of altimeter versus GIM difference (figure 48), the amplitude of the difference is stronger for Sentinel-6 MF than Jason-3. This behavior can be linked to the reduced smoothing in Sentinel-6 MF ionosphere correction filtering, thus giving more accurate reflection of the peaks and troughs in the ionospheric content.
The NR standard deviation is slightly lower (7.9mm) than in MLE4 (8.0mm), as shown on the right panel of figure 47.

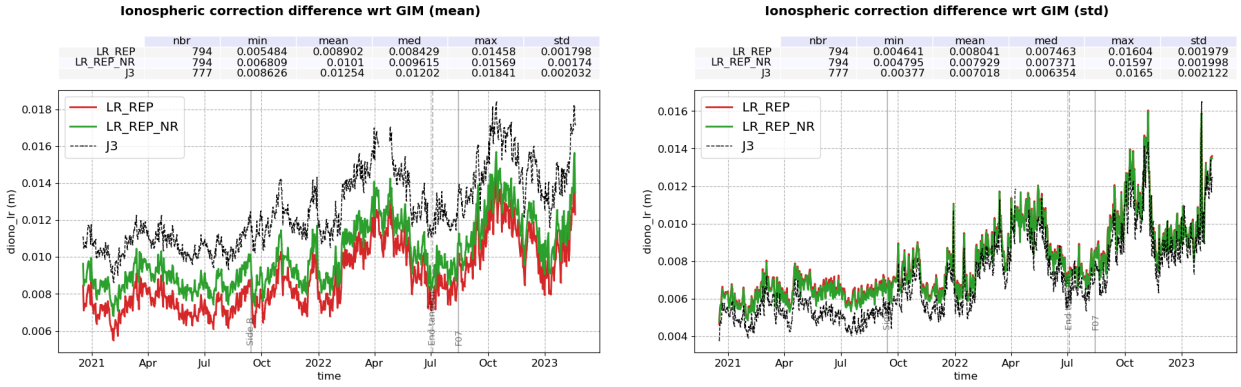

Figure 47 – Time monitoring of the ionosphere correction difference : Altimeter Filtred minus GIM model (m), for Jason-3 (black) and Sentinel-6 MF LR reprocessed data (red for MLE4, green for NR). ***Left*** *: mean per day,* ***right*** *: standard deviation per day.*

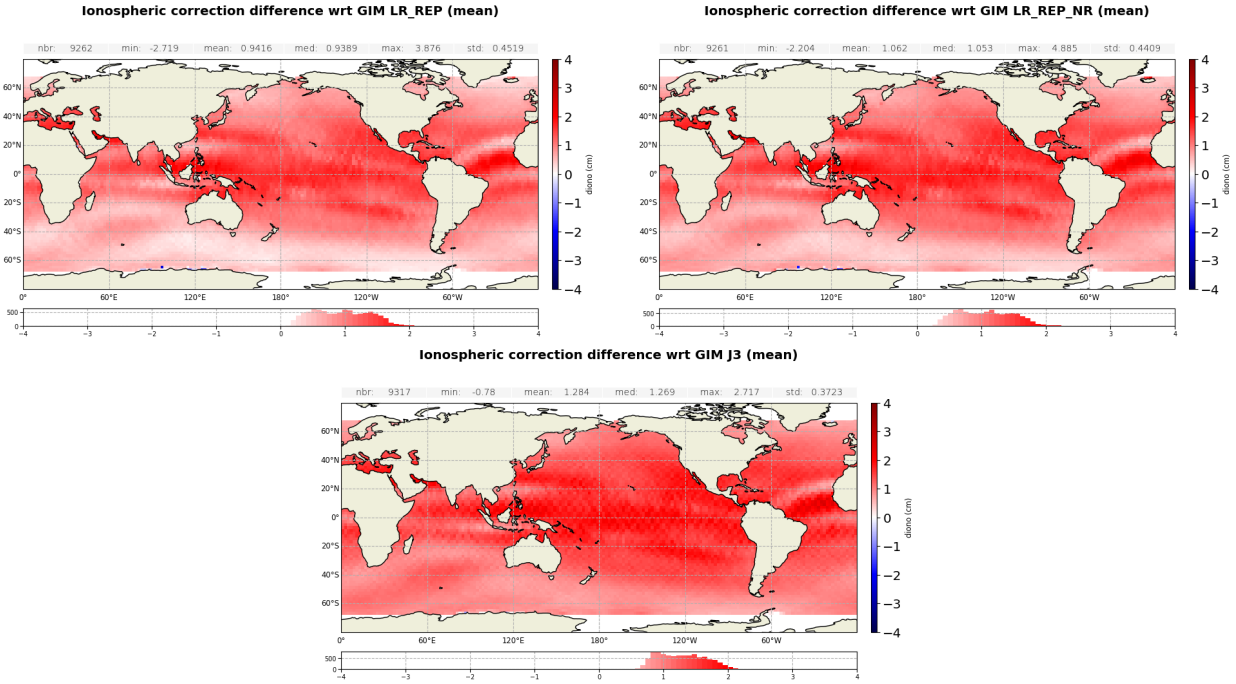

Figure 48 – Map of ionosphere correction difference : Altimeter filtred minus GIM model (m). For Sentinel-6 MF LR reprocessed MLE4 (left), NR (right) and Jason-3 (bottom). Computed over the completed reprocessed period.

4.1.7. Mispointing

In this section is analysed the square of the off-nadir angle derived from LR waveform using MLE4 and NR retrackings. The time series are presented on figure 49 and the distributions, on figure 50. The reprocessing improves the estimation of the mispointing from waveform in MLE4 thanks to the PB F08 antenna aperture update, decreasing from 0.012deg^2 to 0.008deg^2. NR square off-nadir angle is even closer to zero, with a distribution centred on 0.004deg^2. Spikes in the time series are related to cross-manoeuvres.

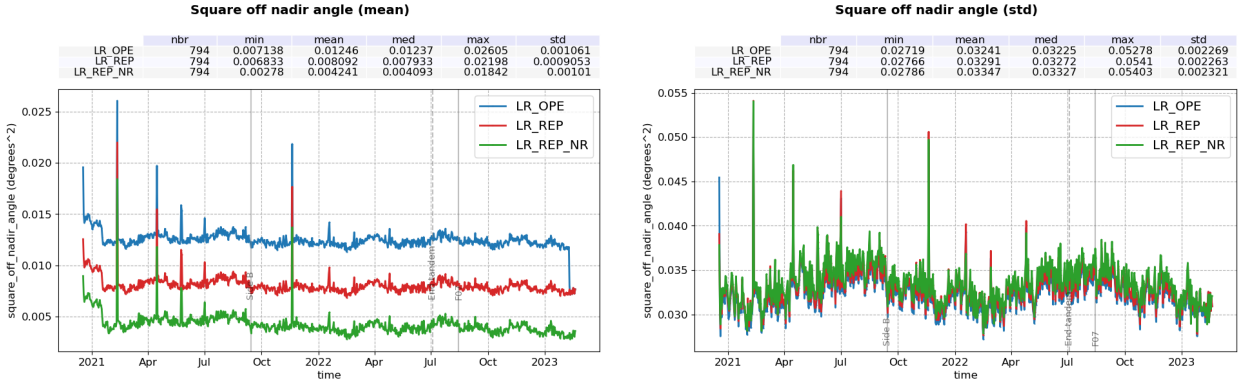

Figure 49 – Time monitoring of square of the off-nadir mispointing angle in deg^2, before reprocessing (blue) and after reprocessing (red). Left: mean per cycle, Right: standard deviation per cycle

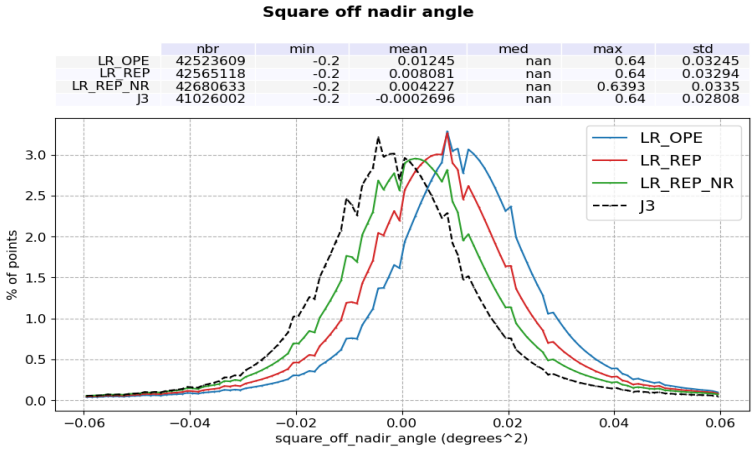

Figure 50 – Histogram of square of the off-nadir mispointing angle for Jason-3 (black) and reprocessed S6 MF LR. Computed over the completed reprocessed period.

While the square off-nadir angle follow similar variations in all datasets, a difference in behaviour has been identified between NR and MLE4 retrackings. Figure 51 shows the mean (left panel) and standard deviation (right panel) MLE4 - NR mispointing difference as a function of MLE4 mispointing. The differences are insignificant at low mispointing but increase rapidly beyond 0.2deg^2. At very high mispointing, the differences are beyond 50%. The standard deviation of the differences also increases with the mispointing.

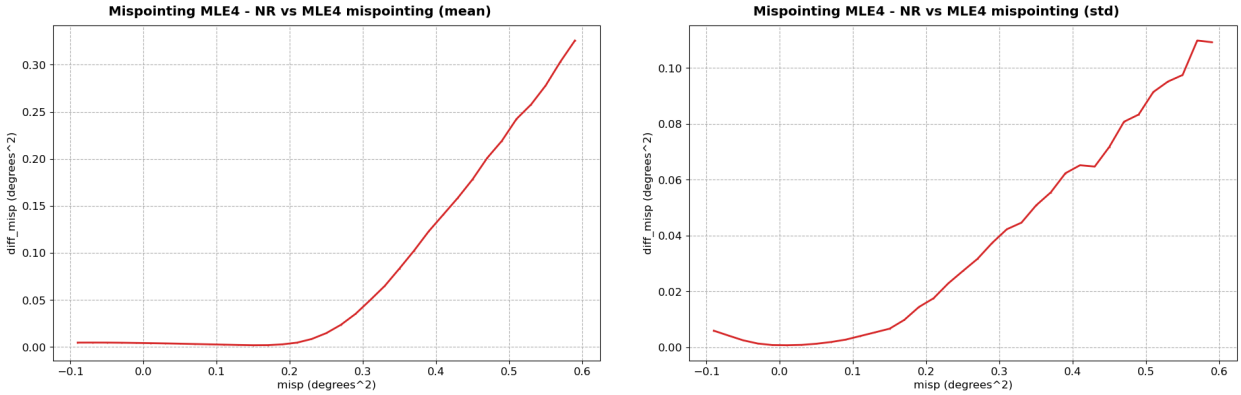

Figure 51 – Sentinel-6 MF LR reprocessed MLE4 - NR square off-nadir angle differences as a function of the reprocessed MLE4 square off-nadir angle. Left : mean, right : standard deviation.

The high differences in mispointing impact other retracking outputs, namely backscatter coefficient and the range (figure 52). The sea surface height anomaly (SSHA) is also impacted. These impacts are far from negligible and go up to -0.75dB for the sigma0, 12cm for the range and 9cm on the SSHA.

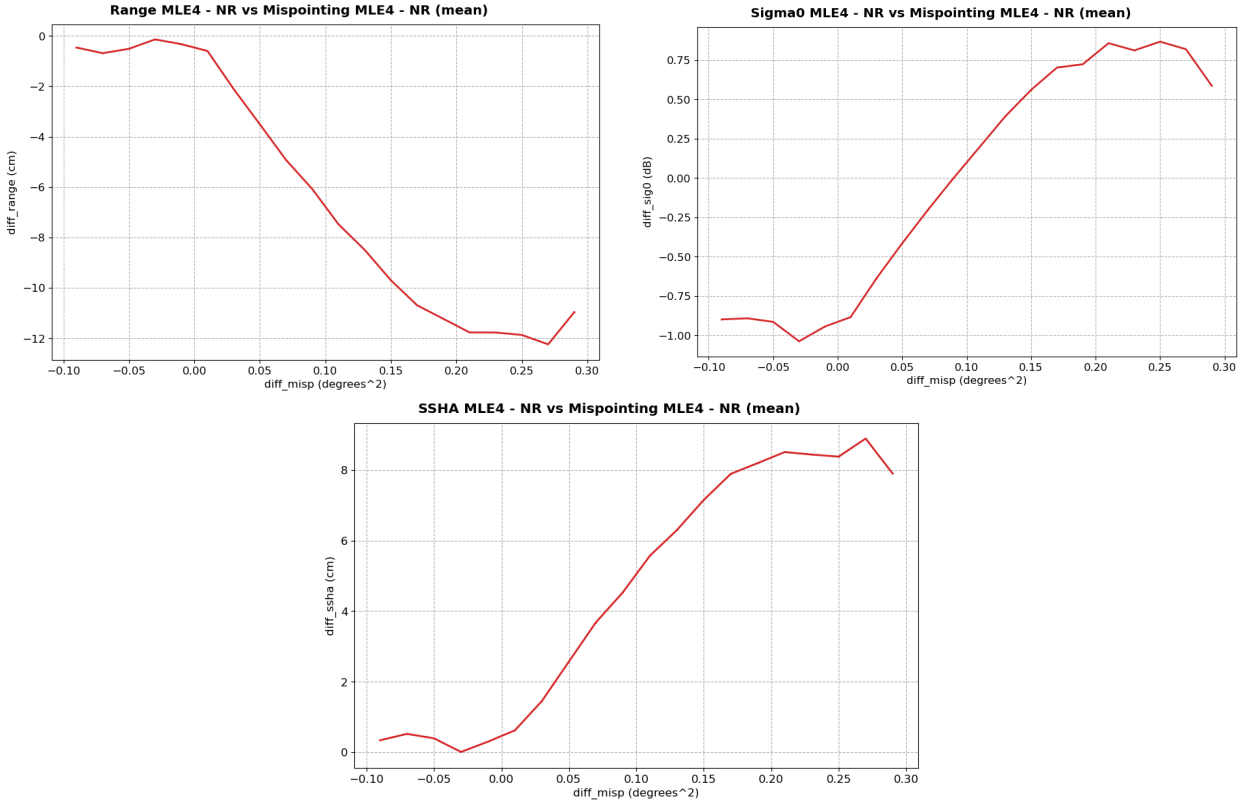

*Figure 52 – Sentinel-6 MF LR reprocessed MLE4 - NR range (**left**), sigma0 (**right**) and SSHA (**bottom**) mean differences as a function of the reprocessed MLE4 - NR square off-nadir angle differences.*

While this difference in behavior is insignificant during normal operations, it has a noticeable impact during

satellite manoeuvres with high mispointing. Figure 53 presents an example on cycle 44 pass 4 (2022-01-18), which contains two yaw slew manoeuvres (-90 and +90 degrees respectively). In this instance, NR - MLE4 difference reaches -0.24deg^2 in mispointing, 20cm in range and SSHA, and 1.5dB in sigma0. This unexpected difference in behavior is under investigation.

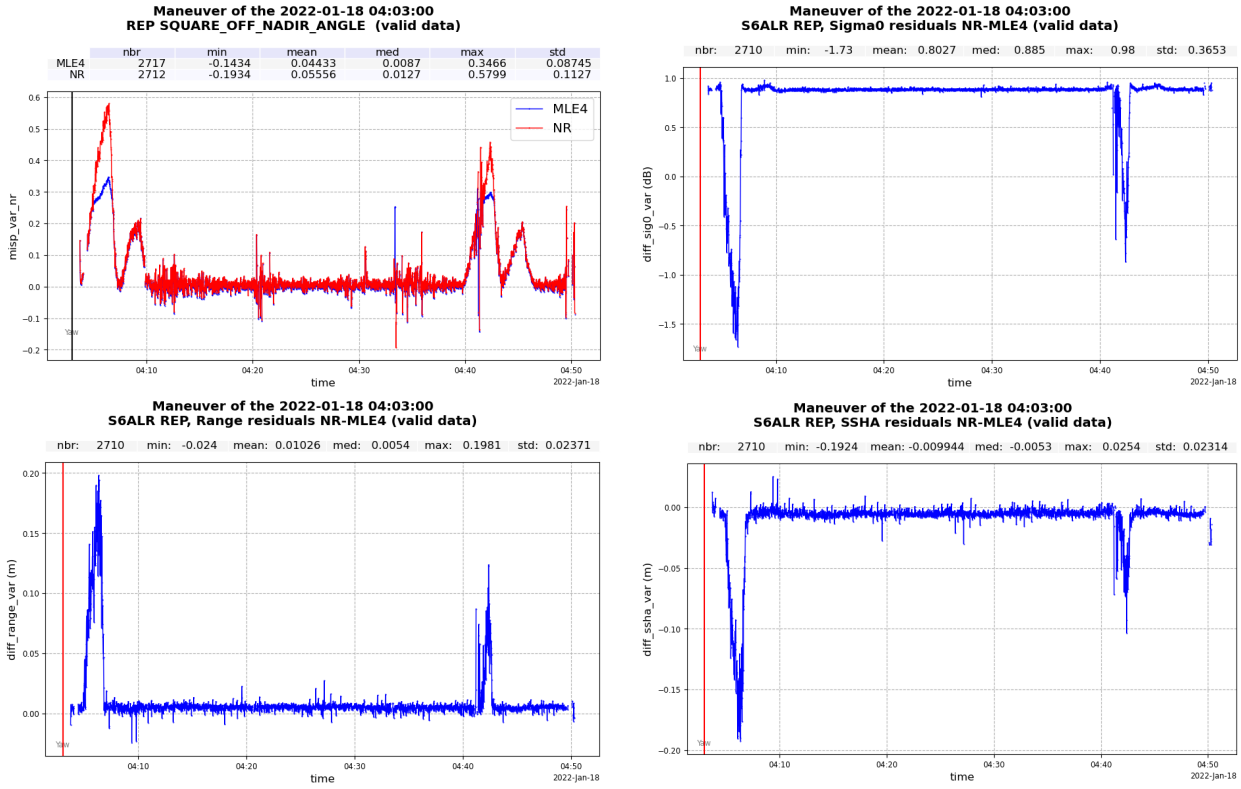

*Figure 53 – Sentinel-6 MF along-track reprocessed MLE4 (blue) and NR (red) square off-nadir angle (**top left**) and reprocessed NR - MLE4 sigma0 (**top right**), range (**bottom left**) and SSHA (**bottom right**) for cycle 44 pass 4.*

4.2. Wet tropospheric correction from radiometer

4.2.1. Differences between operational and reprocessed WTC

The mean difference between operational and reprocessed WTC is presented on figure 54, left panel. Differences are mostly stable, with two main drifts :

- Between 2021-04-22 and 2021-05-04, with a maximum amplitude of about -1.5mm, directly following a POS-4 restart and ending with a +1.5mm jump back to previous levels. The cause of this drift is unknown at the time of writing.
- Between 2022-10-01 and 2022-12-14. This drift has been identified as resulting from a calibration error in the microwave radiometer in operational data. On 2022-12-14, the error was fixed, causing a jump of about +5.5mm back to previous levels. This drift has been completely corrected in reprocessed data.

Additionally, three main regime changes are observed. First, both WTC are identical up until 2021-02-03 (cycle 8 pass 214). Then they show stable differences, centred around about -0.2mm. Starting from March 2022, the differences increase and vary with time, reaching amplitudes of about +/- 1mm. Finally, after the correction of radiometer drift on 2022-12-14, both WTC become identical again. The reasons behind these changes are still under investigations.

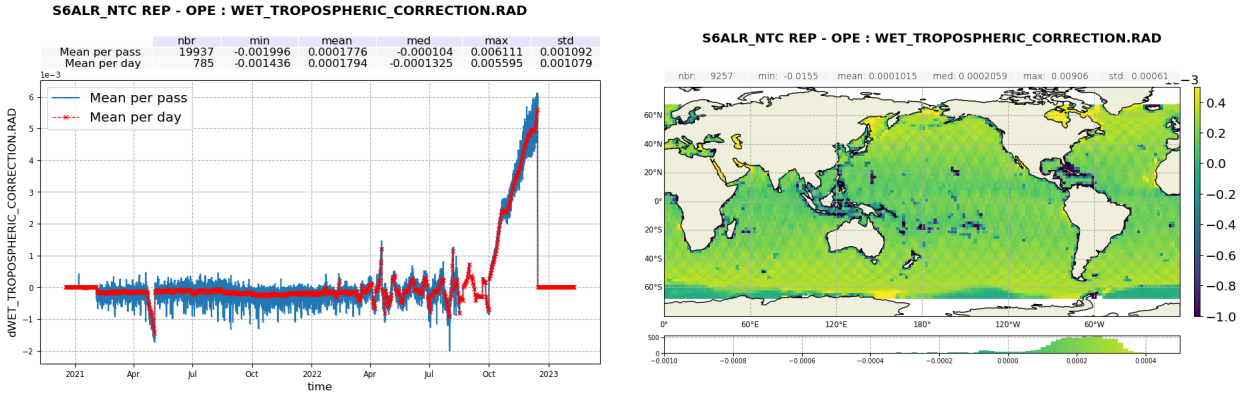

*Figure 54 – Monitoring (**left**) per day (red) and pass (blue) and map (**right**) of the reprocessed - operational LR WTC difference*

The map of these differences is presented on the right panel of figure 54. The most significant differences are located in coastal areas. This is due to the inclusion of HRMR in addition of AMR-C in the WTC computation which improved coastal performances in the PB F07 update.

4.2.2. Differences between radiometer and model WTC

Monitoring of the differences between radiometer and model WTC allows to highlight any jump or drift between the two retrievals and is presented on figure 55. The mean differences curves follow similar variations for operational and reprocessed datasets, except for the two drifts described in the previous section. Three phases are visible, induced by two events (figure 55 left panel):

- On 27-28 April 2021, a jump of -4 mm is observed in the bias preceded by a progressive increase of the bias (from beginning of March 2021) by the same amplitude. The jump visible on 27-28 April 2021 is concomitant with a satellite restart and is not observed in Jason-3 time series. The amplitude of

the jump is higher by about 1mm in the reprocessed dataset. The potential link between the satellite restart and this jump is under investigation.

- On 13 October 2021, a jump of +2 mm is observed on both Sentinel-6 MF and Jason-3 monitoring. It is linked to an update in the ECMWF model (see [6] for more details).

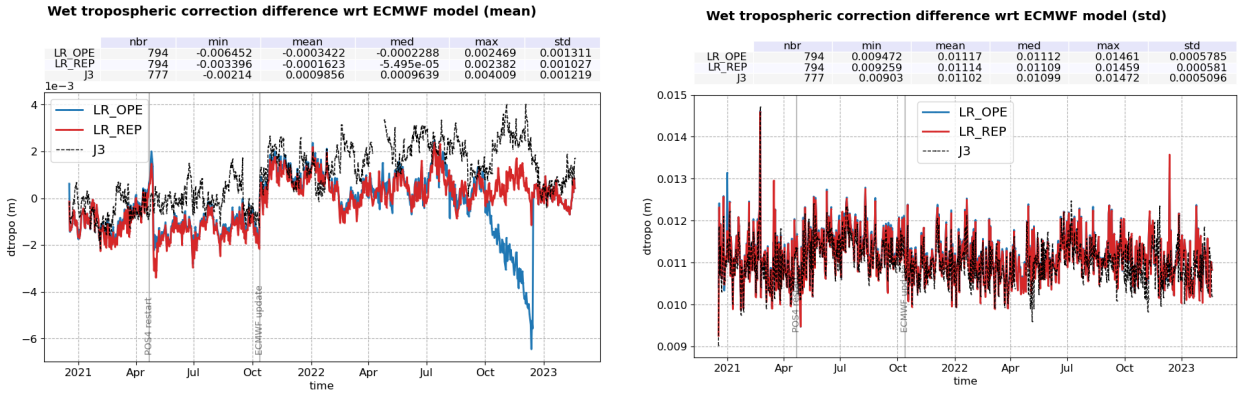

*Figure 55 – Time monitoring of wet tropospheric correction difference (m): WTC from radiometer minus WTC from ECMWF model. Before reprocessing (blue), after reprocessing (red) and for Jason-3 (black). **Left**: mean per day, **Right**: standard deviation per day*

After reprocessing, Sentinel-6 MF radiometer WTC is slightly closer the the ECMWF model with an average bias of -0.16mm (from -0.34mm) see figure 56. The bias is also smaller than that of Jason-3 (0.97mm).

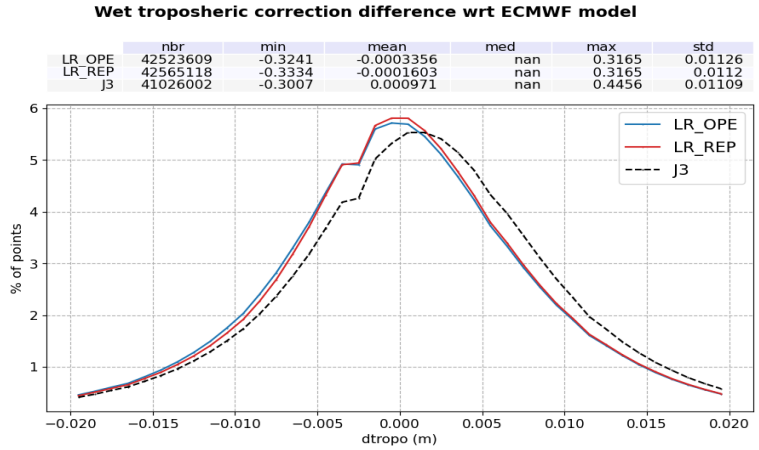

Figure 56 – Histogram of radiometer WTC for Jason-3 (black) and reprocessed Sentinel-6 MF. Computed over the completed reprocessed period.

The corresponding maps (figure 57) do not highlight strong discrepancies between Sentinel-6 MF and Jason-3 retrievals.

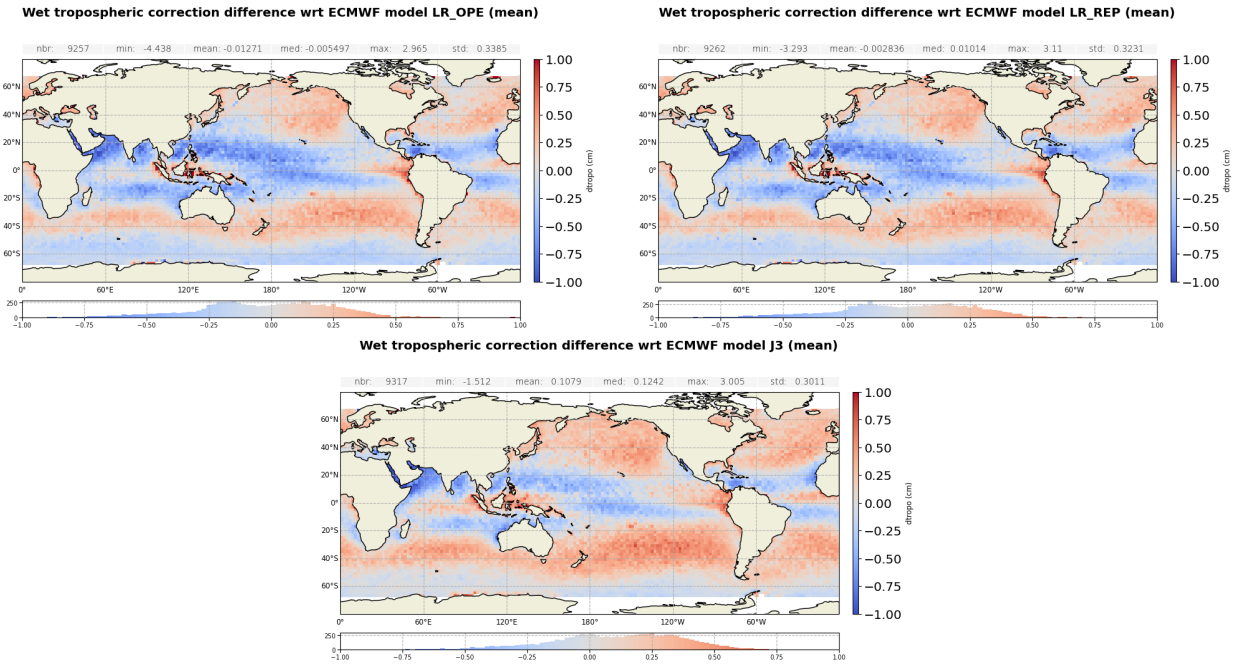

*Figure 57 – Map of WTC difference : Radiometer minus ECMWF model (m). For Sentinel-6 MF operational dataset (**left**), reprocessed dataset (**right**) and Jason-3 (**bottom**). Computed over the completed reprocessed period.*

4.3. Sea Level Performances

The Sea Surface Height Anomaly (SSHA) is the most well-known parameter estimated from altimetry. It corresponds to the elevation of sea surface, with respect to a reference called Mean Sea Surface (MSS), generated by oceanic variability and climatic phenomena (such as Gulf Stream current, El Nino, ...). It is computed as follows:

$$SSHA = Orbit - AltimeterRange - \sum(GeophysicalCorrections) - MeanSeaSurface$$

The details of the geophysical corrections can be found in Sentinel ALT Level 2 Product Generation Specification [7].

4.3.1. Along-track analysis

4.3.1.1. LR

The monitoring of Sentinel-6 MF LR SSHA is presented on figure 58. As the filtered ionosphere correction and therefore the SSHA became available on the Caspian Sea only after the PB F07 update, the Caspian Sea was removed in this figure for a better comparison with the PB F06 segment of operational data. Besides the correction of the WTC drift from October to December 2021 (see section 4.2.), no significant difference in variations is visible between operational and reprocessed MLE4 SSHA. Corresponding maps on figure 59 do not highlight any significant regional difference.

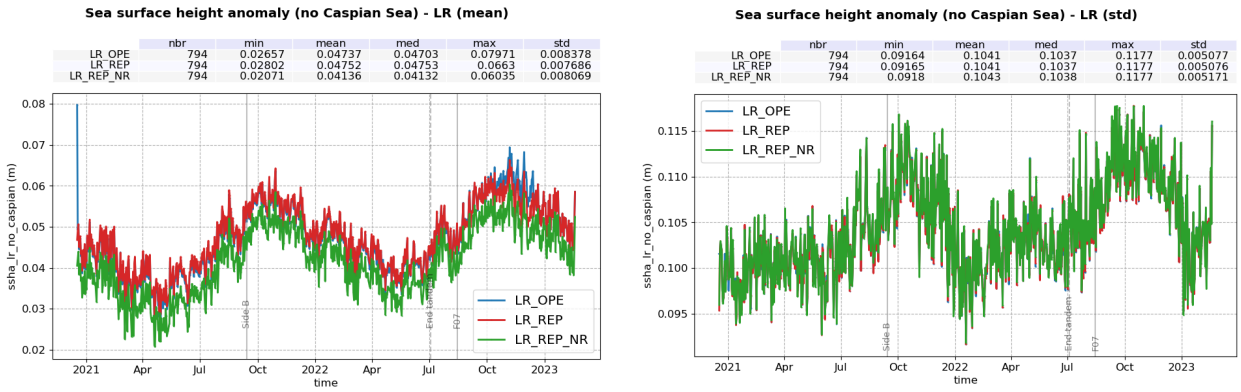

Figure 58 – Time monitoring of Sentinel-6 MF SSHA in meters, without the Caspian Sea, before reprocessing (blue) and after reprocessing (red for MLE4, green for NR). ***Left****: mean per day,* ***Right****: standard deviation per day.*

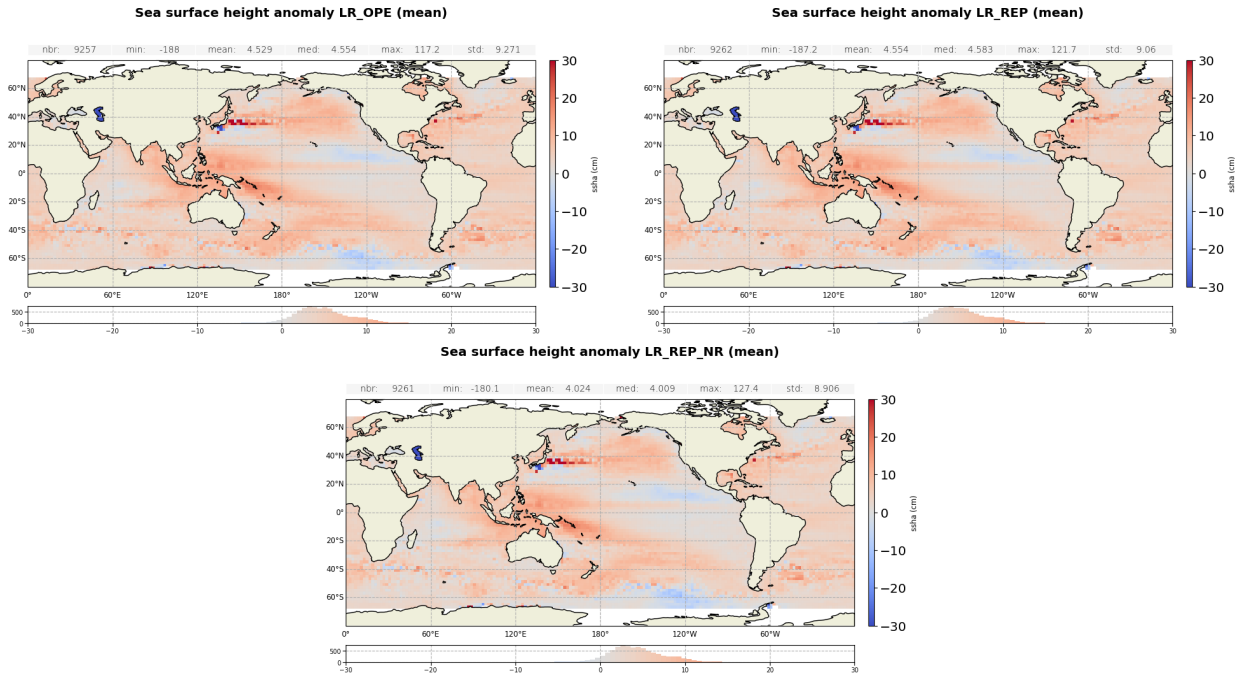

*Figure 59 – Maps of Sentinel-6 MF LR SSHA in meters for operational MLE4 (**left**), reprocessed MLE4 (**right**) and NR (**bottom**).*

MLE4 operational vs reprocessed

The MLE4 reprocessed - operational differences (figure 60) are mostly stable in time, except for the two drifts related to the WTC and described in section 4.2.. After the last jump on 2022-12-14, differences are negligible. The corresponding map (right panel) show significant coastal differences due to the inclusion of HRMR data in WTC with the PB F07 update (see section 4.2.).

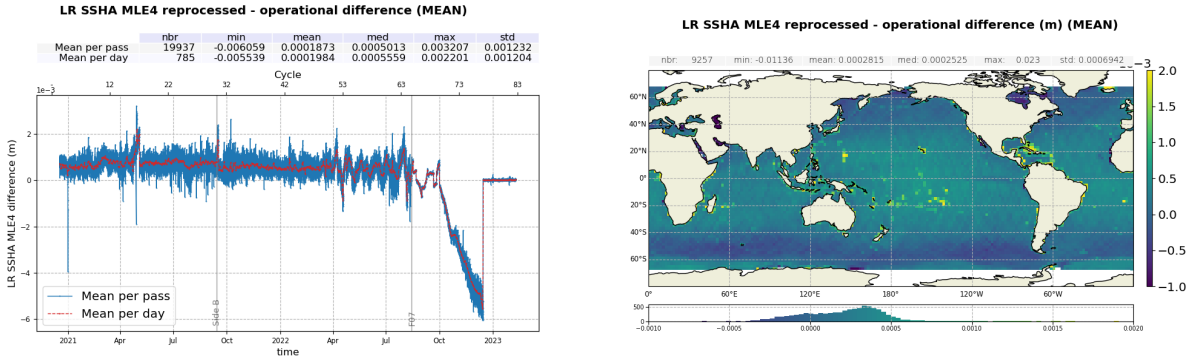

*Figure 60 – Map (**right**) and time monitoring (**left**) of Sentinel-6 MF LR MLE4 operational - reprocessed SSHA in meters per day (red) and per pass (blue).*

Reprocessed MLE4 vs NR

The reprocessed NR - MLE4 SSHA differences monitoring on figure 61 shows an about 1.5mm jump at side B switch, resulting from range (section 4.1.2.1.) and ionosphere correction behaviours (section 4.1.6.). The corresponding map on figure 62 highlights a significant SWH correlation, with about -1.5cm decrease between 0.5 and 8m-SWH. This behavior is expected and is part of the improvement brought by the numerical retracker. Indeed, contrary to MLE4, numerical retracker outputs are not corrected by instrumental LUTs, which are applied function of SWH values. Numerical retracker retrievals are then less sensitive to any approximation in the LUT estimation. Analysis performed in the frame of Sentinel-6 MF commissioning activities have shown that part of the residual bias between S6 MF LR MLE4 and J3 can be attributed to S6 MF instrumental LUT. Using numerical retracker strongly reduces the correlation to SWH in S6 MF LR/J3

SSHA bias. More details about this improvement will be added in the next version of this report, in the tandem phase analysis section.

The standard deviation of the SSHA difference is degraded at low SWH which is probably linked to the anomaly in negative SWH management in LR NR (see section 2.1.).

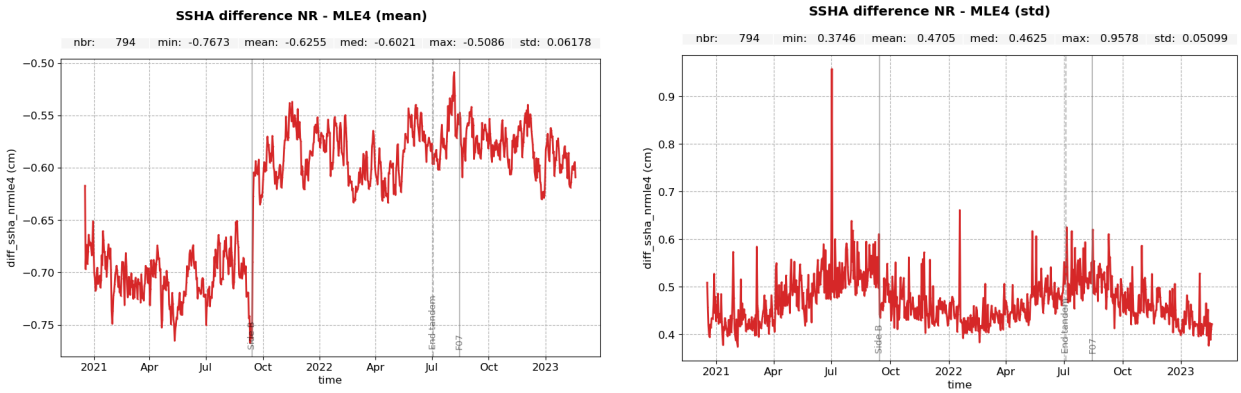

*Figure 61 – Time monitoring of Sentinel-6 MF reprocessed NR - MLE4 SSHA in meters, without the Caspian Sea, before reprocessing (blue) and after reprocessing (red for MLE4, green for NR). **Left**: mean per day, **Right**: standard deviation per day.*

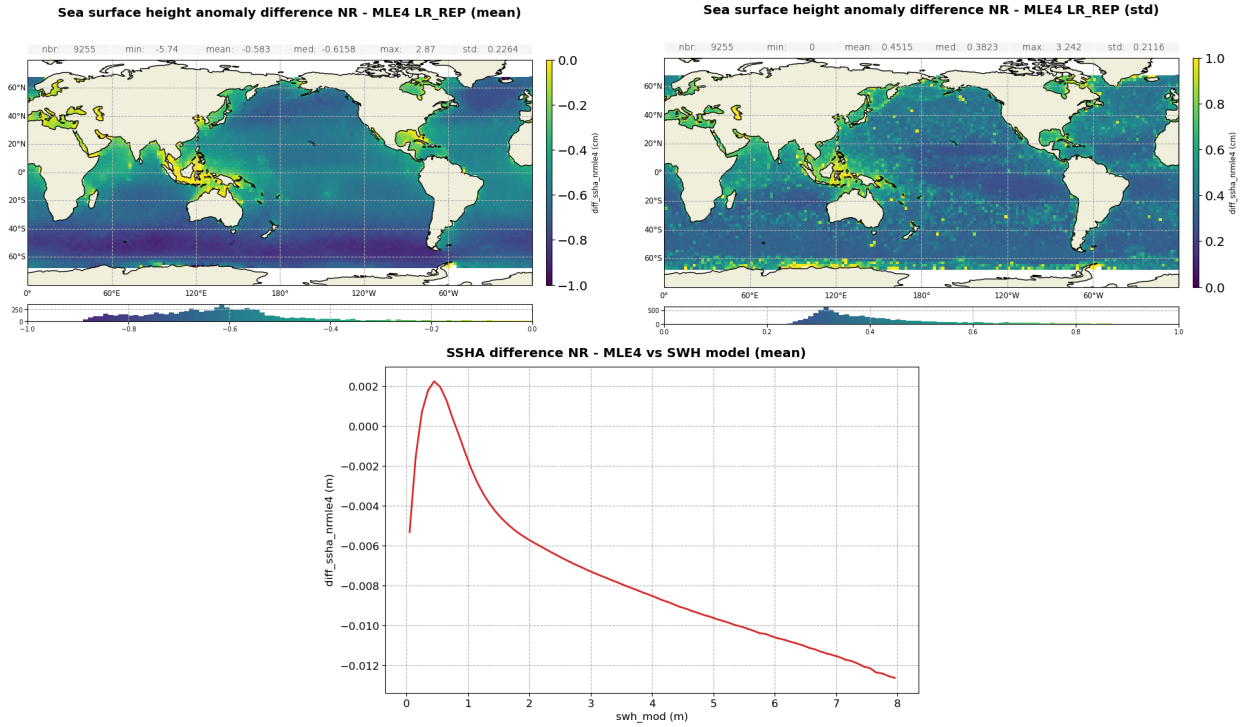

*Figure 62 – Maps of mean (**left**) and standard deviation (**right**) of Sentinel-6 MF LR reprocessed NR - MLE4 SSHA in meters, and its mean as a function of ERA 5 model SWH (**bottom**).*

The NR - MLE4 SSHA distributions are presented on figure 63 for side A (left panel) and side B (right panel). SSHA are consistent between both retrackings, with only a -7.0mm bias on side A and -5.8mm on side B.

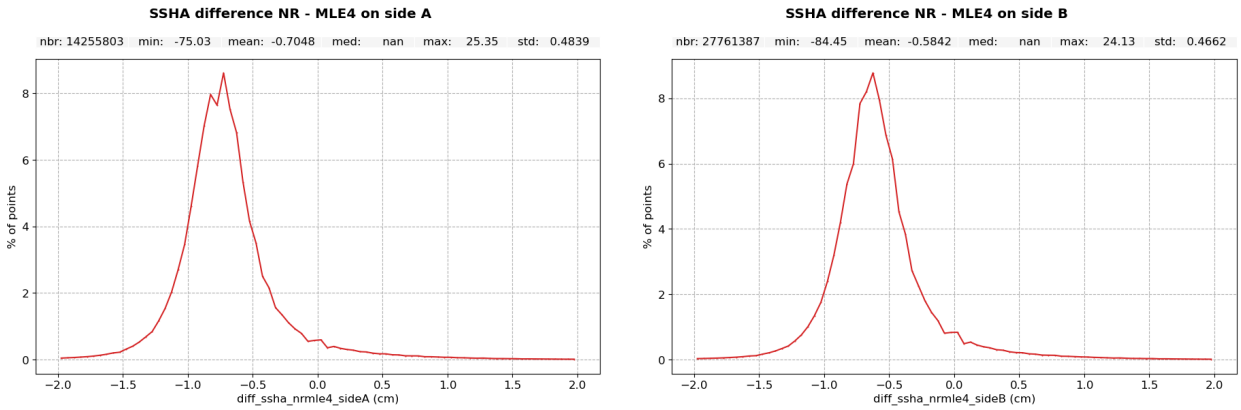

*Figure 63 – Distributions of Sentinel-6 MF F08 NR - MLE4 SSHA difference for side A (**left**) and side B (**right**).*

4.3.1.2. HR

The HR reprocessed - operational differences (figure 64) are mostly stable in time, except for the two drifts related to the WTC and described in section 4.2.. The corresponding map (right panel) shows significant coastal differences due to the inclusion of HRMR data in WTC with the PB F07 update (see section 4.2.).

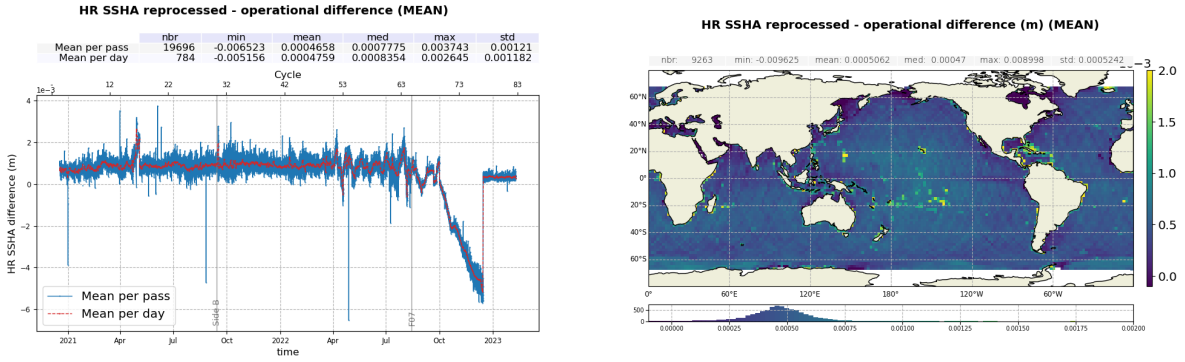

*Figure 64 – Map (**right**) and time monitoring (**left**) of Sentinel-6 MF HR operational - reprocessed SSHA in meters per day (red) and per pass (blue).*

4.3.1.3. HR - LR

HR versus LR MLE4 SSHA bias is monitored in figure 65. The bias is reduced by about 0.2mm with the reprocessing (-1.15cm vs -1.17cm). A drift of -1mm/year is seen in both datasets, and is related to the range walk correction not yet applied in HR mode. On side A, both curves are more in line than on side B, pointing to the existence of a small jump difficult to observe due to the day-to-day variations of SSHA measurements. A marginal decrease in SWH correlation (right panel) is observed with the reprocessing. This dependency with SWH comes from the skewness coefficient being set to 0 on HR side whereas is it set to 0.1 on LR.

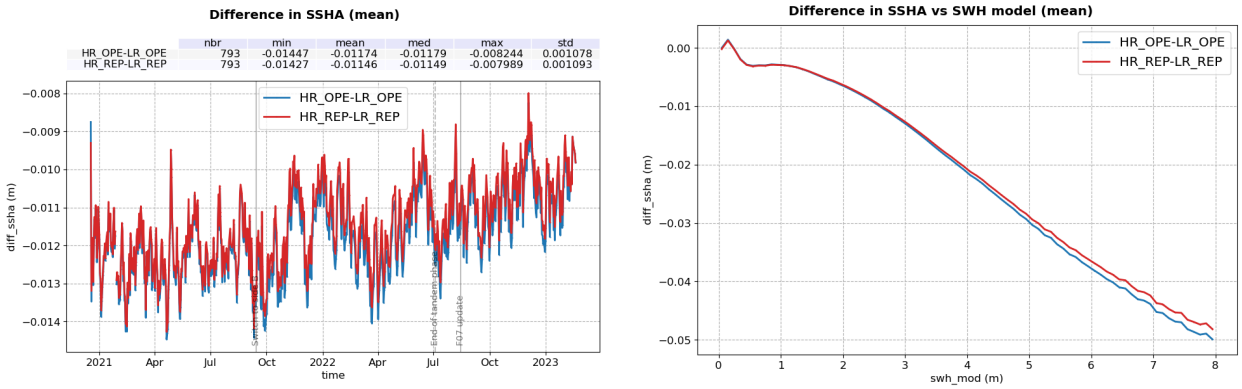

*Figure 65 – Time monitoring (**left**) and ERA 5 model SWH dependency (**right**) of Sentinel-6 MF SSHA difference : HR - LR MLE4, before reprocessing (blue) and after reprocessing (red)*

4.3.2. Crossover analysis

Sea Surface Height crossover differences are the SSH differences between ascending and descending passes where they cross each other. Crossover differences are systematically analyzed to estimate data quality and the Sea Surface Height (SSH) performances. SSH crossover differences are computed from the valid data set on a one cycle basis, with a maximum time lag of 10 days, in order to limit the effects of ocean variability which are a source of error in the performance estimation. The mean SSH crossover differences should ideally be close to zero and standard deviation should ideally be small.

Nevertheless, SLA varies also within 10 days, especially in high variability areas. Furthermore, due to lower data availability (due to seasonal sea ice coverage), models of several geophysical corrections are less precise in high latitude. Therefore, an additional geographical selection - removing shallow waters, areas of high oceanic variability and high latitudes ($> |50|$ deg) - is applied for cyclic monitoring.

Table 6 summarizes the mean and standard deviation of the SSH difference at crossovers across all datasets. The reprocessing had a negligible impact on mean SSH difference at crossover, as seen in the cyclic monitoring presented on figure 66 for all Sentinel-6 MF datasets and Jason-3. Looking at standard deviation of the SSH difference at crossovers (figure 67), operational and reprocessed LR datasets present similar performance. In HR, differences are also insignificant except for three spikes in the reprocessed dataset on cycles 32, 57 and 61. These spikes are of unknown origins and do not appear in the monitoring of the standard deviation of HR SSHA.

Dataset	Mean (cm)	STD (cm)
S6 MF LR MLE4 operational	-0.02	4.71
S6 MF LR MLE4 reprocessed	-0.02	4.71
S6 MF LR NR reprocessed	-0.02	4.68
S6 MF HR operational	0.08	4.48
S6 MF HR reprocessed	0.07	4.50
Jason-3	-0.03	4.65

Table 6 – Mean and standard deviation of SSH difference at crossovers

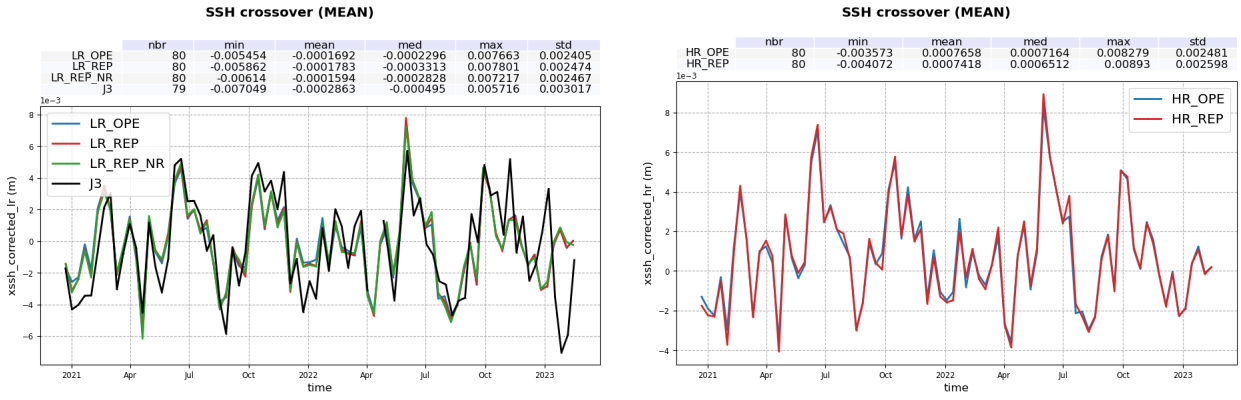

Figure 66 – Monitoring of the mean of SSH difference at mono-mission crossover for each cycle in meters. ***Left*** *: LR and Jason-3.* ***Right*** *: HR.*

Maps of LR SSH difference at crossovers are smooth and do not highlight any strong discrepancies between ascending and descending tracks in terms of SSH (figure 68).

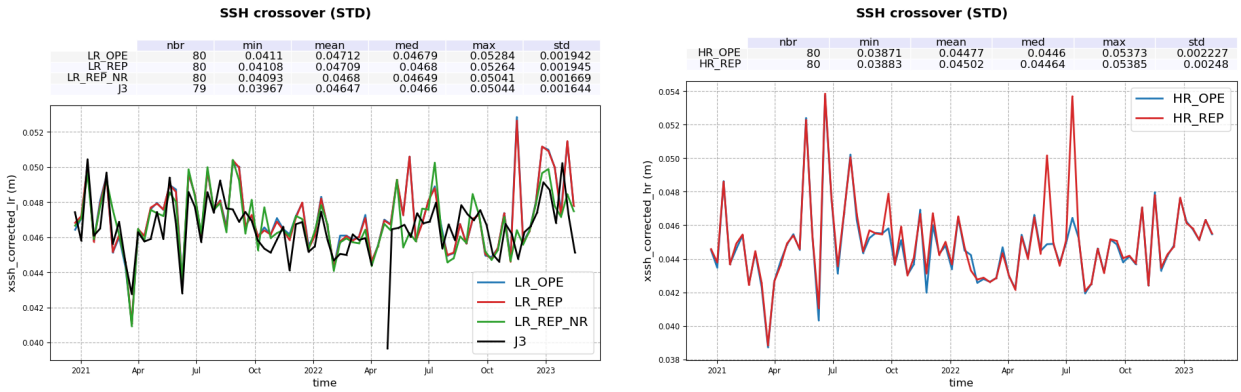

*Figure 67 – Monitoring of the standard deviation of SSH difference at mono-mission crossover for each cycle in meters. **Left** : LR and Jason-3. **Right** : HR.*

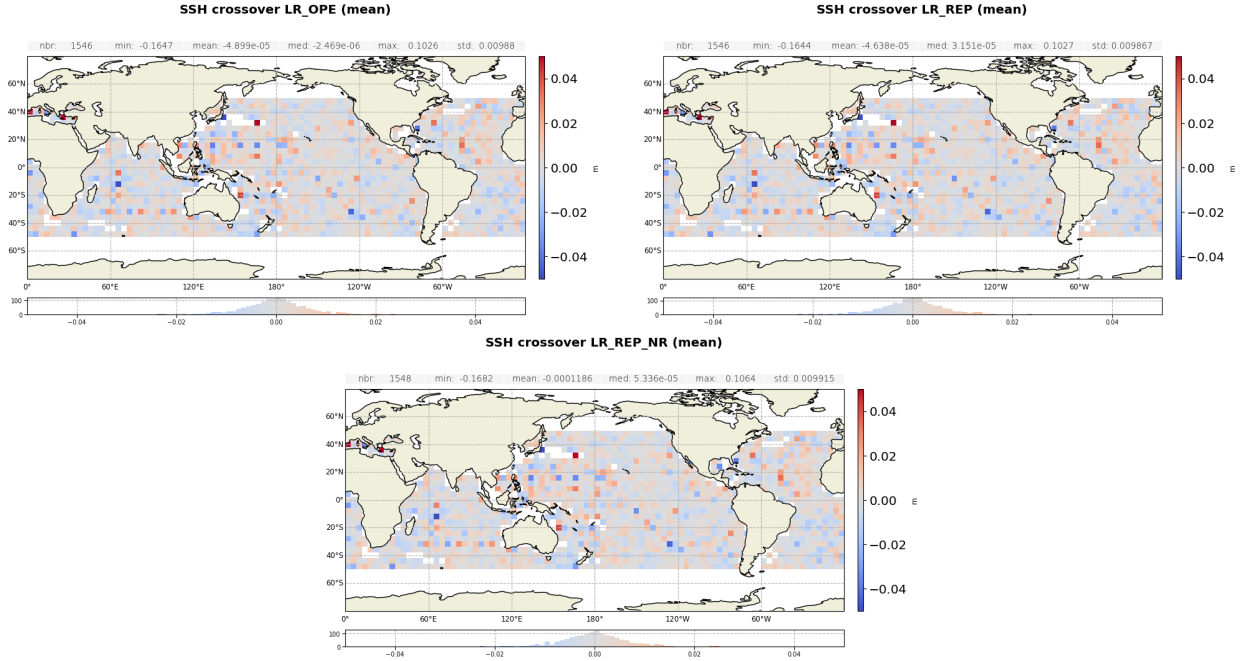

*Figure 68 – Mean SSH difference at crossovers for Sentinel-6 MF LR operational MLE4 (**top left**), reprocessed MLE4 (**top right**) and NR (**bottom**). Computed over the complete reprocessing period.*

Maps of HR SSH difference at crossovers highlight patterns correlated to along-track wind (figure 69). It is linked to the residual impact of along-track wind on HR data and more particularly on HR range.

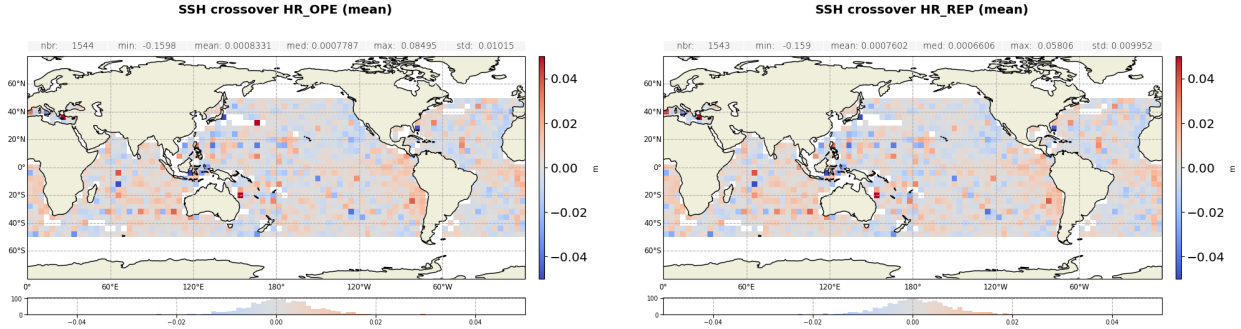

*Figure 69 – Mean SSH difference at crossovers for Sentinel-6 MF HR operational data (**left**) and reprocessed data (**right**). Computed over the complete reprocessing period.*

5 Conclusion

An overview of the impact of Sentinel-6 MF F08 reprocessing over ocean has been presented in this report. The Processing Baseline F08 used for this reprocessing brought two major improvements:

- The update of POS4 antenna aperture from 1.33° to 1.34°, to improve mispointing estimation. In LR MLE4, mispointing value is reduced from 0.012deg^2 to 0.008deg^2.
- The addition of LR Numerical Retracker retrievals, in order to better account for system aging (PTR shape evolution).

This numerical retracker brings significant improvements on the range long term evolution, as seen the HR versus LR range evolution. This improvement will be further quantified in the GMSL analysis, available in the upcoming version of this report foreseen for September 2023. Also, the dependency of LR range to SWH variations is strongly reduced thanks to numerical retracking. Contrary to MLE4, NR accounts for all instrumental behaviours in real time. Therefore, it does not require approximate instrument corrections (e.g. LUTs). It brings a strong improvement in the consistency between Jason-3 and Sentinel-6 MF in terms of range and thus SSHA (detailed in the upcoming version of this report).

An anomaly (AR 2620) has been raised on the handling of small waves with the numerical retracking which introduced biases at low SWH. This anomaly will be patched at the end of summer 2023 in operational data through a correction of the 20Hz to 1Hz compression. Other unexpected differences with MLE4 are still being investigated, such as residual SWH bias at high SWH, sensitivity to sea surface slope and behaviour at high mispointing.

This reprocessing also includes improvements brought by PB F07 on data before 2022-08-15 :

- The availability of High Resolution Microwave Radiometer (HRMR) data in all radiometer products, improving WTC at the coast
- The usage of ECHO CAL as main source of CAL1.
- An update of the ionospheric correction filtering method. With this update, the filtered ionospheric correction became available over the Caspian Sea in the products, enabling SSHA computation in this region.

With this reprocessing, a significant -2mm/month drift impacting the wet tropospheric correction from October to December 2022 has also been corrected.

The impact of the reprocessing is small in other aspects, with submillimetric differences in geophysical parameters such as SWH, range, SSB, or SSHA, for both LR MLE4 and HR datasets. Performances of the SSH difference at crossovers remain similar with operational data.

For its second version, this report will be completed by three additional parts :

- An analysis of Sentinel-6 MF consistency to Jason-3 over the tandem phase.
- An analysis of the reprocessing impact on Sentinel-6 MF GMSL.
- A compliance status to system requirements.

6 References

References

[1] Sentinel-6A F06 Reprocessing Calval Assesment available at : https://www-cdn.eumetsat.int/files/2022-10/S6A_F06_Reprocessing_Calval_Assesment_v2_draft4.pdf

[2] Sentinel-6A user handbook available at https://eumetsatspace.atlassian.net/wiki/spaces/SEN6/overview

[3] Sentinel-6A product notice for Processing Baseline F08 at https://www.eumetsat.int/media/50743

[4] Sentinel-6A product notice for Processing Baseline F07 at https://www.eumetsat.int/media/50079

[5] Jason-3 product handbook available at https://www.aviso.altimetry.fr/fileadmin/documents/data/tools/hdbk_j3.pdf

[6] Changes in ECMWF model, web page: https://www.ecmwf.int/en/forecasts/documentation-and-support/changes-ecmwf-model

[7] Sentinel ALT Level 2 Product Generation Specification available at https://www.eumetsat.int/media/48266

[8] Raynal et al, Lessons learned from Sentinel SARM missions in preparation of Jason-CS. Oral Presentation, Ocean Surface Topography Science Team Meeting 2019, Chicago